

Water wave scattering by a step of arbitrary profile

By R. PORTER¹ AND D. PORTER²

¹School of Mathematics, University of Bristol, Bristol, BS8 1TW, UK

²Department of Mathematics, The University of Reading, P. O. Box 220, Whiteknights,
Reading, RG6 6AX, UK

(Received 12 October 1999 and in revised form 16 December 1999)

The two-dimensional scattering of water waves over a finite region of arbitrarily varying topography linking two semi-infinite regions of constant depth is considered. Unlike many approaches to this problem, the formulation employed is *exact* in the context of linear theory, utilizing simple combinations of Green's functions appropriate to water of constant depth and the Cauchy–Riemann equations to derive a system of coupled integral equations for components of the fluid velocity at certain locations. Two cases arise, depending on whether the deepest point of the topography does or does not lie below the lower of the semi-infinite horizontal bed sections. In each, the reflected and transmitted wave amplitudes are related to the incoming wave amplitudes by a scattering matrix which is defined in terms of inner products involving the solution of the corresponding integral equation system.

This solution is approximated by using the variational method in conjunction with a judicious choice of trial function which correctly models the fluid behaviour at the free surface and near the joins of the varying topography with the constant-depth sections, which may not be smooth. The numerical results are remarkably accurate, with just a two-term trial function giving three decimal places of accuracy in the reflection and transmission coefficients in most cases, whilst increasing the number of terms in the trial function results in rapid convergence. The method is applied to a range of examples.

1. Introduction

The problem of water wave scattering by a bed of arbitrary shape is of considerable interest to coastal engineers and, despite its long history, it continues to receive much attention. This is the case even for two-dimensional scattering using linearized theory, which we consider here.

As only one exact solution has been found, by Roseau (1976) for a specific bed shape, a variety of techniques have been developed to approximate the scattering process. The essential difficulties posed by the problem, which these techniques seek to overcome by one means or another, are that the governing differential equation (Laplace's) is elliptic and the domain is of an arbitrary shape and is unbounded.

One approach which has enjoyed some success reduces the dimension of the problem, by approximating the vertical motion of the fluid and implementing an averaging process which entirely removes the vertical coordinate. In particular, Laplace's equation is replaced by an ordinary differential equation when the technique is applied to two-dimensional scattering problems. This method, which requires that the bed

shape be slowly-varying, relative to the local wavelength, is the basis of the mild-slope equation derived independently by Berkhoff (1972, 1976) and Smith & Sprinks (1975). Kirby (1986) derived a variant of the mild-slope equation and applied it to the problem of Bragg resonance by ripple beds and, more recently, Chamberlain & Porter (1995) have developed another enhanced version of the mild-slope equation, the modified mild-slope equation, which has a wider range of applicability than its predecessors. These various equations are concerned only with the contribution to the scattering process of the propagating waves. A further extension of the same basic idea which includes the effect of an arbitrary number of evanescent modes has been described by Massel (1993) and by Porter & Staziker (1995). Athanassoulis & Belibassakis (1999) have recently proposed an alternative way of including evanescent modes using a coupled-mode theory. A similar coupled-mode technique has been adopted in the formulation of scattering problems in hydroacoustics involving variable-width acoustic waveguides (see, for example, Rutherford & Hawker 1981; Fawcett 1992 and Boyles 1984). However, in all such examples, the condition on the assumed slowly-varying part of the waveguide is only approximately satisfied.

A quite different approximation method in which the given bed profile is replaced by a sequence of horizontal shelves joined at vertical steps has its origins in an application of localization theory to surface waves given by Devillard, Dunlop & Souillard (1988). The technique exploits the simpler problem of scattering by a vertical step joining two semi-infinite horizontal bed sections, which we shall encounter later. The limitations of topography discretization have been explored by O'Hare & Davies (1991), Rey (1992) and Guazzelli, Rey & Belzons (1992).

Evans & Linton (1994), building on the work of Fitz-Gerald (1976), have recently developed an alternative discretization method, in which the fluid strip is mapped into one of uniform width. The bed shape manifests itself as a variable coefficient in the revised free-surface boundary condition and the discretization follows on approximating this coefficient by a piecewise-constant function. Restrictions on the bed slope imposed by direct topography discretization do not arise, as Evans & Linton illustrate by considering the case in which the bottom profile consists of an isolated vertical barrier on an otherwise horizontal bed.

Yet another way of dealing with scattering follows by formulating the problem as an integral equation or an integral equation system. In principle at least, this method offers the greatest prospect of accuracy as the governing equations and the given bed shape are used exactly, the approximation arising only in solving the integral equation problem. In particular, the approach reduces the dimension of the problem, which is the key feature of the mild-slope equation and its variants, but it does so without invoking an approximation which limits its applicability. The method depends on the availability of one or more Green's functions which correspond to the given topography, in the sense that their use results in integral equations posed on bounded domains and of a type for which economical and accurate computational methods are available. Surprisingly, this technique has only recently been used to calculate scattering by a localized elevation on a horizontal bed, by Staziker, Porter & Stirling (1996). The appropriate Green's function in this case is that corresponding to a fluid of constant depth, leading to an integral equation on the elevation. Liu & Liggett (1982) had previously used the simpler fundamental solution of Laplace's equation rather than this Green's function. To avoid integral equations on infinite intervals (the free surface and the whole of the bed), they applied Green's identity to a bounded domain, encompassing a local elevation, for example, and matched the resulting representation of the potential with truncated separation solutions, valid outside

the bounded domain. The boundary element method was used to approximate the solution in the finite domain and determine the coefficients in the separation solutions. Liu & Liggett (1982) and Mei (1978) give comprehensive reviews of the use of the boundary element method in water wave problems.

The scattering problem in which an arbitrary profile joins two semi-infinite horizontal bed sections at different depths is more interesting, from the point of view of applications, than that involving an elevation of bounded extent on a single horizontal bed. It is also a more difficult problem from the integral equation point of view, although one to which the mild-slope equation, topography discretization and the Evans & Linton (1994) mapping method may be applied. Evans (1972) formulated an integral equation over the arbitrary profile, by determining the Green's function corresponding to a semi-infinite shelf set at an arbitrary level in water of uniform depth. However, the complicated nature of this Green's function, obtained by the Wiener–Hopf method, seems to preclude a numerical solution of the resulting integral equation.

In the present work we adopt a fresh approach to the general problem considered by Evans (1972), but one which is also founded on integral equation techniques. To see the way forward, we note that a class of scattering problems which is simpler than the one we have in hand is that in which the topography consists of line segments, each of which is parallel to one or other of the coordinate lines. The vertical-step problem referred to earlier can be regarded as the canonical problem in this category. The simplification occurs because the domain of the problem consists of the union of rectangular subdomains on each of which appropriate separation solutions can be derived. Matching these solutions at the common boundaries of the subdomains leads directly to integral equations of a type for which powerful solution techniques exist. Miles (1967) and, more recently, Porter (1995) have used this approach for the vertical-step water-wave problem and subsequently Evans & Fernyhough (1995) and Fernyhough & Evans (1995) have adapted the method of Porter (1995) to problems in acoustics involving rectangular geometries. Related problems in acoustics have also been solved by the expansion matching method by Evans & Linton (1991), using systems of algebraic equations rather than the equivalent integral equations.

We base our solution method on the same general idea and find that, with the aid of some judicious manipulation, we can preserve the essential structure found for rectangular geometries, in the case of a general bed profile. The matching of separation solutions is no longer available, but we can use Green's functions defined on appropriate rectangular regions, and match representations of the potential given by applying Green's identity on corresponding subdomains. We emphasize that the conditions of linear theory are all satisfied exactly in the formulation we adopt including the no-flow condition on the bed. A key part of the process is the way in which the integral contribution along the arbitrary profile is handled. By using the Cauchy–Riemann equations to replace normal derivatives of functions by tangential derivatives of other functions, on the profile, we can preserve the inherent symmetry of the Green's functions and this ultimately leads us to self-adjoint integral equation systems in which the kernels are at most logarithmically singular.

Two cases arise in the implementation of our approach, depending on whether the bed profile does or does not extend below the level of the lower of the two semi-infinite horizontal sections. In both cases we obtain a structure reminiscent of that encountered by Porter (1995) for rectangular geometries. Thus, to determine the scattered wave amplitudes, which is our aim, we have to calculate the values of inner products $\langle \mathbf{q}^{(i)}, \mathbf{f}_j \rangle$ for $i, j = 1, 2$, where $\mathbf{q}^{(1)}$ and $\mathbf{q}^{(2)}$ satisfy self-adjoint operator

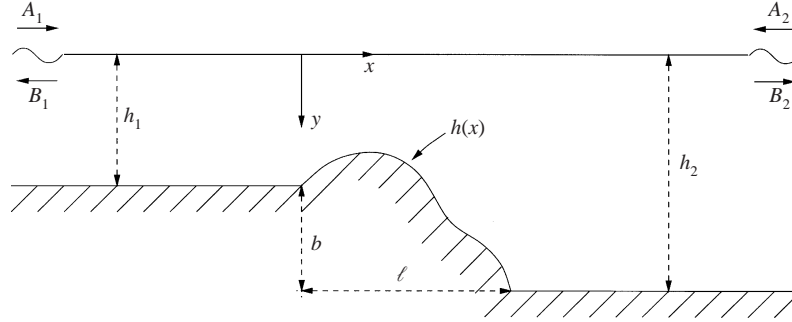


FIGURE 1. Schematic of the topography.

equations of the form $\mathbf{K}\mathbf{q}^{(i)} = \mathbf{f}_i$ for $i = 1, 2$, defined on composite Hilbert spaces. Highly accurate estimates of these inner products are obtained by extending standard variational methods to our problem and using these in conjunction with prudently chosen approximations to $\mathbf{q}^{(i)}$. We remark that piecewise-constant approximations could be taken for these unknown functions, somewhat in the spirit of topography discretization, but we can do better by modelling properties of the exact solutions more closely.

We formulate the problem and carry out the basic groundwork in the following section, before addressing the two cases cited above in §§ 3 and 4. The approximation method and associated numerical issues are discussed in § 5, and finally, in § 6, a selection of results is presented.

2. Formulation and preliminaries

As we are concerned only with two-dimensional scattering, we work with Cartesian coordinates (x, y) (see figure 1). These are arranged so that y is measured vertically downwards, $y = 0$ coinciding with the undisturbed free surface. The bed is given by $y = H(x)$ for $-\infty < x < \infty$, where

$$H(x) = \begin{cases} h_1, & x < 0, \\ h(x), & 0 \leq x \leq \ell, \\ h_2, & \ell < x, \end{cases} \quad (2.1)$$

h_1 and h_2 being constants. The function $h(x) > 0$ is continuous for $0 \leq x \leq \ell$, with $h(0) = h_1$ and $h(\ell) = h_2$, and it has continuous derivative for $0 < x < \ell$. Thus $H(x)$ is continuous everywhere but the bed slope $H'(x)$ may be discontinuous at $x = 0$ and $x = \ell$. For definiteness we take $h_2 > h_1$ and maintain generality by allowing waves, of given angular frequency ω , to be incident from both $x = -\infty$ and $x = \infty$.

According to linear water wave theory, the velocity potential Φ which describes the motion can be written as

$$\Phi(x, y, t) = \text{Re} \{ \phi(x, y) e^{-i\omega t} \}$$

where ϕ satisfies

$$\nabla^2 \phi \equiv \phi_{xx} + \phi_{yy} = 0 \quad \text{in } D: -\infty < x < \infty, 0 < y < H(x), \quad (2.2)$$

$$\phi_y + K\phi = 0 \quad \text{on } y = 0, -\infty < x < \infty \quad (2.3)$$

with $K = \omega^2/g$ (g is acceleration due to gravity),

$$\phi_y = 0 \quad \text{on} \quad \begin{cases} y = h_1, & x < 0, \\ y = h_2, & x > \ell, \end{cases} \quad (2.4)$$

and

$$\phi_n = 0 \quad \text{on} \quad C: 0 < x < \ell, y = h(x), \quad (2.5)$$

the subscript n denoting the outward normal derivative from D on C .

We also have to specify the far-field behaviour of ϕ . It is easily shown by separating variables that we may take

$$\begin{aligned} \phi(x, y) &\sim -\{A_1 e^{ik_1 x} + B_1 e^{-ik_1 x}\} \psi_{1,0}(y), & x \rightarrow -\infty, \\ &\sim \{A_2 e^{-ik_2 x} + B_2 e^{ik_2 x}\} \psi_{2,0}(y), & x \rightarrow \infty, \end{aligned} \quad (2.6)$$

where k_i denotes the positive real root of

$$K = k_i \tanh k_i h_i \quad (2.7)$$

for $i = 1, 2$ and we have anticipated later notation by writing

$$\begin{aligned} \psi_{i,0}(y) &= N_{i,0}^{-1/2} \cosh k_i (h_i - y), \\ N_{i,0} &= \frac{1}{2} \{1 + \sinh(2k_i h_i)/2k_i h_i\}, \end{aligned} \quad (2.8)$$

also for $i = 1, 2$.

The complex amplitudes A_1 and A_2 of the incoming waves are assumed to be given and the scattered wave amplitudes B_1 and B_2 are to be determined. If the waves are incident from $x = -\infty$ only and are of unit amplitude, $A_2 = 0$ and the amplitudes of the reflected and transmitted waves are $R_1 = B_1/A_1$ and $T_1 = -B_2/A_1$, respectively. Correspondingly, for unit-amplitude waves travelling from $x = +\infty$ only, the reflected wave amplitude is $R_2 = B_2/A_2$ and the transmitted wave amplitude is $T_2 = -B_1/A_2$. It follows that, in the general case given by (2.6),

$$\begin{pmatrix} B_1 \\ B_2 \end{pmatrix} = \mathbf{S} \begin{pmatrix} A_1 \\ A_2 \end{pmatrix}, \quad \mathbf{S} = \begin{pmatrix} R_1 & -T_2 \\ -T_1 & R_2 \end{pmatrix} \quad (2.9)$$

and the scattering matrix \mathbf{S} may be regarded as the principal unknown of the problem.

Porter & Chamberlain (1997) have recently shown that (2.6) implies $\mathbf{S}\bar{\mathbf{S}} = \mathbf{I}$, from which follow the well-known relationships between the components of \mathbf{S} , due originally to Kreisel (1949). These relationships are therefore automatically satisfied by the exact solution of the scattering problem and by an approximation to it which preserves the far-field structure (2.6). One of these relationships is $|R_1| = |R_2|$. Conservation of energy is given by

$$k_1 h_1 (|A_1|^2 - |B_1|^2) = k_2 h_2 (|A_2|^2 - |B_2|^2)$$

and this relationship allows $|T_i|$ to be calculated given knowledge of $|R_i|$, for $i = 1, 2$.

Due to the different depth into which the transmitted wave progresses, the transmission coefficients for the free-surface displacement are recovered by introducing the scaling

$$\tilde{T}_1 = T_1 \psi_{2,0}(0)/\psi_{1,0}(0), \quad \tilde{T}_2 = T_2 \psi_{1,0}(0)/\psi_{2,0}(0)$$

(see Miles 1967).

The boundary-value problem for ϕ is now completely specified. We seek the (unique) solution of (2.2)–(2.6) which is continuous in \bar{D} and infinitely differentiable in D . The

behaviour of $\nabla\phi$ near the points $(0, h_1)$ and (ℓ, h_2) depends on the bed shape $h(x)$ and will need to be investigated as a preliminary to numerical calculations. It is sufficient at this stage to remark that singularities in the first derivatives of ϕ induced by discontinuities in $H'(x)$ are square-integrable. This knowledge allows the integral equations we obtain to be expressed as operator equations in the Hilbert spaces $L_2(0, a)$ for certain values of a .

To implement the solution process described in §1 we must derive integral representations of ϕ on subdomains of D , using Green's functions for rectangular regions. Two cases arise, depending on the magnitude of

$$h_3 = \max_{0 < x < \ell} h(x).$$

If $h_3 = h_2$, two subdomains are required, $x < 0$, $0 < y < H(x)$ and $0 < x$, $0 < y < H(x)$, and the Green's functions used are those for the semi-infinite strips $x < 0$, $0 < y < h_1$ and $0 < x$, $0 < y < h_2$.

However, if $h_2 < h_3$, a further region is needed to accommodate the local depression in the bed. We therefore use the subdomains $x < 0$, $0 < x < \ell$ and $\ell < x$ in this case, with $0 < y < H(x)$ in each case. A further Green's function, defined in $0 < x < \ell$, $0 < y < h_3$ is also required. The assumed boundary at $y = h_3$ is artificial, but serves to provide a realistic limiting case of the problem, in which there is a rectangular trench between two horizontal beds. Of course, the second arrangement of subdomains is the more general and can be used for all $h(x)$, but it is unnecessarily complicated if $h_3 \leq h_2$.

We shall eventually have to consider the two cases $h_3 \leq h_2$ and $h_2 < h_3$ separately but some preliminary work can be carried out before that point is reached.

The various Green's functions we shall need may be deduced from a basic Green's function, G_i say, defined on the infinite strip $-\infty < x < \infty$, $0 < y < h_i$, where h_i is a constant. We therefore let $G = G_i(x, y|x_0, y_0)$ satisfy

$$\nabla^2 G = -\delta(x - x_0)\delta(y - y_0) \quad (2.10)$$

in $-\infty < x < \infty$, $0 < y < h_i$, where $-\infty < x_0 < \infty$, $0 < y_0 < h_i$,

$$G_y + KG = 0 \quad (2.11)$$

on $y = 0$, $-\infty < x < \infty$, and

$$G_y = 0 \quad (2.12)$$

on $y = h_i$, $-\infty < x < \infty$, together with the radiation condition

$$G \sim A_{i\pm}(x_0, y_0)e^{ik_i|x|}\psi_{i,0}(y), \quad x \rightarrow \pm\infty. \quad (2.13)$$

The wavenumber k_i and the function $\psi_{i,0}$ are defined by (2.7) and (2.8) respectively.

It is a routine matter to determine G_i in terms of the set of eigenfunctions obtained by separation of variables in the corresponding homogeneous problem, namely

$$\left. \begin{aligned} \psi_{i,n}(y) &= N_{i,n}^{-1/2} \cos k_{i,n}(h_i - y), \\ N_{i,n} &= \frac{1}{2} \{1 + \sin(2k_{i,n}h_i)/2k_{i,n}h_i\}, \end{aligned} \right\} n = 0, 1, 2, \dots \quad (2.14)$$

We have used $k_{i,n}$ ($n = 1, 2, \dots$) to denote the positive real roots of

$$K = -k_{i,n} \tan k_{i,n}h_i$$

arranged so that $k_{i,n} < k_{i,n+1}$ and we have adopted the notation $k_{i,0} = -ik_i$ to subsume the function $\psi_{i,0}$ given in (2.8) into the definition (2.14). The set $\{\psi_{i,n}\}$ is orthonormal

on the interval $[0, h_i]$ with weight h_i^{-1} , so that

$$\int_0^{h_i} \psi_{i,n}(y)\psi_{i,m}(y)dy = h_i\delta_{mn}, \quad n, m = 0, 1, 2, \dots$$

and it is complete.

We readily find that

$$G_i(x, y|x_0, y_0) = \sum_{n=0}^{\infty} \frac{\psi_{i,n}(y)\psi_{i,n}(y_0)}{2k_{i,n}h_i} e^{-k_{i,n}|x-x_0|}, \quad (x, y) \neq (x_0, y_0) \quad (2.15)$$

and therefore

$$G_i \sim \frac{i\psi_{i,0}(y)\psi_{i,0}(y_0)}{2k_i h_i} e^{ik_i|x-x_0|}, \quad |x-x_0| \rightarrow \infty, \quad (2.16)$$

which implies that $A_{i\pm}(x_0, y_0) = i\psi_{i,0}(y_0)e^{\mp ik_i x_0}/2k_i h_i$ in (2.13).

To obtain the required integral forms of ϕ we use Green's identity

$$\iint_D (\phi \nabla^2 G - G \nabla^2 \phi) dx dy = \int_S \left(\phi \frac{\partial G}{\partial n} - G \frac{\partial \phi}{\partial n} \right) ds, \quad (2.17)$$

where S denotes the boundary of D , s measures the arc-length on S and $\partial/\partial n$ is the outward normal derivative.

The only boundary element which requires particular attention is C , the curve representing the undulating part of the bed. There we have

$$\left. \begin{aligned} \frac{\partial}{\partial n} &= \frac{1}{\sigma(x)} \left(-h'(x) \frac{\partial}{\partial x} + \frac{\partial}{\partial y} \right), \\ \frac{\partial}{\partial s} &= \frac{1}{\sigma(x)} \left(\frac{\partial}{\partial x} + h'(x) \frac{\partial}{\partial y} \right), \end{aligned} \right\} 0 < x < \ell, \quad (2.18)$$

where

$$\sigma(x) = \sqrt{1 + (h'(x))^2}$$

is the scale factor. Here $\partial/\partial s$ is the derivative along C , in the direction of increasing x . We shall also use the (s, n) coordinates to represent a local orthogonal system in the neighbourhood of C and, in particular, apply (2.18) for points off C .

To deal with the normal derivative of a function on C , we make use of the Cauchy–Riemann equations. The functions we have to deal with, which are evident in (2.15), lead us to introduce the new (non-orthogonal) set

$$\chi_{i,n}(y) = N_{i,n}^{-1/2} \sin k_{i,n}(h_i - y), \quad 0 \leq y \leq h_i, \quad n = 0, 1, 2, \dots \quad (2.19)$$

The convention $k_{i,0} = -ik_i$ applies to give

$$\chi_{i,0}(y) = -iN_{i,0}^{-1/2} \sinh k_i(h_i - y).$$

It follows easily using (2.14) and (2.18) that

$$\left. \begin{aligned} \frac{\partial}{\partial s} \psi_{i,n}(y) e^{\pm k_{i,n}x} &= \mp \frac{\partial}{\partial n} \chi_{i,n}(y) e^{\pm k_{i,n}x}, \\ \frac{\partial}{\partial n} \psi_{i,n}(y) e^{\pm k_{i,n}x} &= \pm \frac{\partial}{\partial s} \chi_{i,n}(y) e^{\pm k_{i,n}x}, \end{aligned} \right\} n = 0, 1, 2, \dots \quad (2.20)$$

For $n \geq 1$ these are examples of the Cauchy–Riemann equations, albeit expressed in

terms of hybrid variables. With $n = 0$ the identities are implied by the Cauchy–Riemann equations.

3. Integral equations for a bed with no depression

Here we consider the simpler of the two cases, in which $h_3 = h_2$, and we first derive a suitable representation of $\phi(x, y)$ for $x < 0$. This makes use of the Green's function $G = G_-$ where

$$G_-(x, y|x_0, y_0) = G_1(x, y|x_0, y_0) + G_1(-x, y|x_0, y_0), \quad (3.1)$$

with $x_0 < 0$ and $0 < y_0 < h_1$, which satisfies (2.10) in $x < 0$, $0 < y < h_1$, (2.11) on $y = 0$, $x < 0$ and (2.12) on $y = h_1$, $x < 0$, together with

$$G_{-x} = 0 \quad \text{on} \quad x = 0, 0 \leq y \leq h_1.$$

Applying (2.17) to ϕ and $G = G_-$ on the domain $-X < x < 0$, $0 < y < h_1$, with $-X < x_0 < 0$, and then evaluating the limit $X \rightarrow \infty$ by means of (2.6) and (2.16), we find that

$$\phi(x_0, y_0) = -2A_1 \cos(k_1 x_0) \psi_{1,0}(y_0) + \int_0^{h_1} G_-(0, y|x_0, y_0) \phi_x(0, y) dy, \quad (3.2)$$

$x_0 < 0, 0 < y < h_1.$

Using (2.16) and (3.1) to determine the far-field behaviour of ϕ and comparing the result with (2.6) shows that

$$B_1 = A_1 - \frac{i}{k_1 h_1} \int_0^{h_1} \psi_{1,0}(y) \phi_x(0, y) dy. \quad (3.3)$$

Finally, letting $x_0 \rightarrow 0$ in (3.2) and separating the propagating ($n = 0$) and evanescent ($n \geq 1$) modes in the Green's function leads to

$$\phi(0, y_0) = -(A_1 + B_1) \psi_{1,0}(y_0) + \int_0^{h_1} \sum_{n=1}^{\infty} \frac{\psi_{1,n}(y) \psi_{1,n}(y_0)}{k_{1,n} h_1} \phi_x(0, y) dy, \quad 0 \leq y_0 \leq h_1, \quad (3.4)$$

when (3.3) has been used to simplify the coefficient of $\psi_{1,0}$.

The equations (3.3) and (3.4) have the familiar structure obtained directly by the eigenfunction matching approach (see, for example, Porter 1995). The present method is, of course, required to determine the counterpart of (3.2) in $x_0 > 0$ for which we require the Green's function $G = G_+$ given by

$$G_+(x, y|x_0, y_0) = G_2(x, y|x_0, y_0) + G_2(-x, y|x_0, y_0) \quad (3.5)$$

with $0 < x_0$ and $0 < y_0 < h_2$. G_+ satisfies (2.10) in $0 < x$, $0 < y < h_2$, (2.11) on $y = 0$ for $0 < x$, (2.12) on $y = h_2$ for $0 < x$ and

$$G_{+x} = 0 \quad \text{on} \quad x = 0, 0 \leq y \leq h_2.$$

Using (2.17) on the truncated domain $0 < x < X$, $0 < y < h_2$ and then letting $X \rightarrow \infty$, we obtain

$$\begin{aligned} \phi(x_0, y_0) = & 2A_2 \cos(k_2 x_0) \psi_{2,0}(y_0) \\ & - \int_0^{h_1} G_+(0, y|x_0, y_0) \phi_x(0, y) dy - \int_C \phi(x, y) \frac{\partial}{\partial n} G_+(x, y|x_0, y_0) ds, \end{aligned} \quad (3.6)$$

$0 < x_0, 0 < y_0 < H(x_0).$

Reference to (2.6) and the far-field behaviour (2.16) of G_i shows that

$$B_2 = A_2 - \frac{i}{k_2 h_2} \int_0^{h_1} \psi_{2,0}(y) \phi_x(0, y) dy - \frac{i}{k_2 h_2} \int_C \frac{\partial}{\partial n} (\cos(k_2 x) \psi_{2,0}(y)) \phi(x, y) ds. \quad (3.7)$$

Now the identities (2.20) imply that

$$\frac{\partial}{\partial n} (\cos(k_2 x) \psi_{2,0}(y)) = -i \frac{\partial}{\partial s} (\sin(k_2 x) \chi_{2,0}(y)) \quad (3.8)$$

and we note that the function $\sin(k_2 x) \chi_{2,0}(y)$ vanishes at both ends of C (that is, at $(0, h_1)$ and (ℓ, h_2)). Therefore, following an integration by parts, (3.7) takes the alternative form

$$B_2 = A_2 - \frac{i}{k_2 h_2} \int_0^{h_1} \psi_{2,0}(y) \phi_x(0, y) dy + \frac{1}{k_2 h_2} \int_C \sin(k_2 x) \chi_{2,0}(y) \frac{\partial \phi(x, y)}{\partial s} ds. \quad (3.9)$$

We now seek an equation which parallels (3.4), by letting $x_0 \rightarrow 0$ in (3.6). First we use (2.20) again, to show that

$$\frac{\partial}{\partial n} G_+(x, y|0, y_0) = -\frac{\partial}{\partial s} \sum_{n=0}^{\infty} \frac{\chi_{2,n}(y) \psi_{2,n}(y_0)}{k_{2,n} h_2} e^{-k_{2,n} x} \quad (3.10)$$

and hence, on integration by parts, that

$$\int_C \phi(x, y) \frac{\partial}{\partial n} G_+(x, y|0, y_0) ds = \int_C \sum_{n=0}^{\infty} \frac{\chi_{2,n}(y) \psi_{2,n}(y_0)}{k_{2,n} h_2} e^{-k_{2,n} x} \frac{\partial \phi(x, y)}{\partial s} ds, \quad 0 \leq y_0 \leq h_1. \quad (3.11)$$

The evaluation terms at the end of C vanish because $\chi_{2,n}(h_2) = 0$ and

$$\sum_{n=0}^{\infty} \frac{\chi_{2,n}(h_1) \psi_{2,n}(y_0)}{k_{2,n} h_2} = \begin{cases} 1, & h_1 < y_0 < h_2, \\ 0, & 0 < y_0 < h_1, \end{cases} \quad (3.12)$$

which is established by expanding the function of y_0 on the right-hand side, regarded as an element of $L_2(0, h_2)$, in the complete set $\{\psi_{2,n}\}$.

If we now set $x_0 = 0$ in (3.6), making use of (3.11) and, at the same time, extract the propagating modes from $G_+(0, y|0, y_0)$ and incorporate (3.9), we arrive at

$$\begin{aligned} \phi(0, y_0) &= (A_2 + B_2) \psi_{2,0}(y_0) - \int_0^{h_1} \sum_{n=1}^{\infty} \frac{\psi_{2,n}(y) \psi_{2,n}(y_0)}{k_{2,n} h_2} \phi_x(0, y) dy \\ &\quad - \int_C \left\{ \frac{i \cos(k_2 x)}{k_2 h_2} \chi_{2,0}(y) \psi_{2,0}(y_0) + \sum_{n=1}^{\infty} \frac{\chi_{2,n}(y) \psi_{2,n}(y_0)}{k_{2,n} h_2} e^{-k_{2,n} x} \right\} \frac{\partial \phi(x, y)}{\partial s} ds, \\ &\quad 0 \leq y_0 \leq h_1. \end{aligned} \quad (3.13)$$

Strictly speaking, because the value of the summation in (3.12) is not known at $y_0 = 0$ and $y_0 = h_1$, the equations (3.11) and (3.13) only hold for $0 < y_0 < h_1$. However, as we shall ultimately interpret the integral equations we derive as operator equations in Hilbert space, the fact that their derivation only holds almost everywhere in the given intervals is not significant. Indeed, we can define $\phi(0, y_0)$ at $y_0 = 0$ and $y_0 = h_1$ by (3.13) and this is the practice we have adopted. We shall not draw attention to other instances of the same issue, which often arises in formulations such as this.

One integral equation is now immediate on equating this last version of $\phi(0, y_0)$

with that given by (3.4). We take the opportunity to introduce some new notation at this stage, writing

$$\left. \begin{aligned} q_1(y) &= \phi_x(0, y), & 0 \leq y < h_1, \\ q_2(x) &= \left[\frac{\partial \phi(x, y)}{\partial x} + h'(x) \frac{\partial \phi(x, y)}{\partial y} \right]_{y=h(x)}, & 0 < x < \ell. \end{aligned} \right\} \quad (3.14)$$

Combining (3.4) and (3.13) and noting that $ds = \sigma(x)dx$ for $(x, y) \in C$, we have

$$\int_0^{h_1} k_{11}(y_0, y)q_1(y)dy + \int_0^\ell k_{12}(y_0, x)q_2(x)dx = (A_1 + B_1)\psi_{1,0}(y_0) + (A_2 + B_2)\psi_{2,0}(y_0), \quad 0 \leq y_0 \leq h_1, \quad (3.15)$$

in which the (real-valued) kernels are given by

$$k_{11}(y_0, y) = \sum_{n=1}^{\infty} \left\{ \frac{\psi_{1,n}(y_0)\psi_{1,n}(y)}{k_{1,n}h_1} + \frac{\psi_{2,n}(y_0)\psi_{2,n}(y)}{k_{2,n}h_2} \right\} \quad (3.16)$$

and

$$k_{12}(y_0, x) = \frac{i}{k_2 h_2} \psi_{2,0}(y_0) \chi_{2,0}(h(x)) \cos(k_2 x) + \sum_{n=1}^{\infty} \frac{\psi_{2,n}(y_0) \chi_{2,n}(h(x))}{k_{2,n} h_2} e^{-k_{2,n} x}. \quad (3.17)$$

To obtain a second equation linking q_1 and q_2 we return to (3.6) and impose the bed condition $\partial \phi(x_0, y_0) / \partial n_0 = 0$ for (x_0, y_0) on C . (We have used an obvious extension of the notation given in (2.18).) Some preparation is needed before we can implement this step.

We first note from (2.15) and (2.20) that, if $(x, y) \neq (x_0, y_0)$,

$$\frac{\partial^2}{\partial n_0 \partial n} G_+(x, y | x_0, y_0) = -\frac{\partial^2}{\partial s_0 \partial s} H_+(x, y | x_0, y_0), \quad (3.18)$$

where

$$H_+(x, y | x_0, y_0) = \sum_{n=0}^{\infty} \frac{\chi_{2,n}(y) \chi_{2,n}(y_0)}{2k_{2,n} h_2} \{ e^{-k_{2,n}|x-x_0|} - e^{-k_{2,n}|x+x_0|} \}. \quad (3.19)$$

This transfer of normal derivatives of G_+ to tangential derivatives of H_+ is a crucial step and has been anticipated by introducing the corresponding manipulation into the derivation of (3.15). In addition to (3.18) we make further use of (3.8) and (3.10) (with the variables x and x_0 , and so on, interchanged) to deduce from (3.6) that

$$\frac{\partial \phi(x_0, y_0)}{\partial n_0} = -\frac{\partial}{\partial s_0} \left\{ 2iA_2 \sin(k_2 x_0) \chi_{2,0}(y_0) - \int_0^{h_1} \sum_{n=0}^{\infty} \frac{\chi_{2,n}(y_0) \psi_{2,n}(y)}{k_{2,n} h_2} e^{-k_{2,n} x_0} \phi_x(0, y) dy - \int_C \frac{\partial}{\partial s} H_+(x, y | x_0, y_0) \phi(x, y) ds \right\}.$$

Enforcing the zero normal flow condition and integrating therefore gives

$$\begin{aligned} \int_0^{h_1} \sum_{n=0}^{\infty} \frac{\chi_{2,n}(y_0) \psi_{2,n}(y)}{k_{2,n} h_2} e^{-k_{2,n} x_0} \phi_x(0, y) dy - \int_C H_+(x, y | x_0, y_0) \frac{\partial \phi(x, y)}{\partial s} ds \\ = 2iA_2 \sin(k_2 x_0) \chi_{2,0}(y_0) + \text{constant}, \quad (x_0, y_0) \in C, \end{aligned} \quad (3.20)$$

where $H_+(0, h_1|x_0, y_0) = 0$ and $H_+(\ell, h_2|x_0, y_0) = 0$ have been used in the integration by parts. The constant of integration is readily found to be zero by letting $(x_0, y_0) \rightarrow (\ell, h_2)$. Finally, we reorganize (3.20) by extricating purely imaginary terms from the kernels, using (3.9) to simplify the result of this process, and by using the notation (3.14). We thus arrive at the integral equation

$$\int_0^{h_1} k_{21}(x_0, y)q_1(y)dy + \int_0^\ell k_{22}(x_0, x)q_2(x)dx = (A_2 + B_2)i \sin(k_2x_0)\chi_{2,0}(h(x_0)),$$

$$0 \leq x_0 \leq \ell, \quad (3.21)$$

in which

$$k_{21}(x_0, y) = k_{12}(y, x_0) \quad (3.22)$$

is defined by (3.17) and

$$k_{22}(x_0, x) = \frac{\chi_{2,0}(h(x_0))\chi_{2,0}(h(x))}{2k_2h_2} \{ \sin(k_2|x - x_0|) - \sin(k_2(x + x_0)) \}$$

$$- \sum_{n=1}^{\infty} \frac{\chi_{2,n}(h(x_0))\chi_{2,n}(h(x))}{2k_{2,n}h_2} \{ e^{-k_{2,n}|x-x_0|} - e^{-k_{2,n}(x+x_0)} \}. \quad (3.23)$$

The velocity components q_1 and q_2 are determined by the coupled equations (3.15) and (3.21). As our aim is to calculate the scattering matrix \mathbf{S} defined in (2.9), the equations (3.3) and (3.9) are also significant, expressed in the forms

$$\left. \begin{aligned} B_1 &= A_1 - \frac{i}{k_1h_1} \int_0^{h_1} \psi_{1,0}(y)q_1(y)dy, \\ B_2 &= A_2 - \frac{i}{k_2h_2} \int_0^{h_1} \psi_{2,0}(y)q_1(y)dy + \frac{1}{k_2h_2} \int_0^\ell \sin(k_2x)\chi_{2,0}(h(x))q_2(x)dx. \end{aligned} \right\} \quad (3.24)$$

In order to expose the structure of the key equations we adopt a more succinct notation. We introduce the operators K_{ij} defined by

$$\left. \begin{aligned} (K_{11}q_1)(y_0) &= \int_0^{h_1} k_{11}(y_0, y)q_1(y)dy, \\ (K_{12}q_2)(y_0) &= \int_0^\ell k_{12}(y_0, x)q_2(x)dx, \end{aligned} \right\} \quad 0 \leq y_0 \leq h_1,$$

$$\left. \begin{aligned} (K_{21}q_1)(x_0) &= \int_0^{h_1} k_{21}(x_0, y)q_1(y)dy, \\ (K_{22}q_2)(x_0) &= \int_0^\ell k_{22}(x_0, x)q_2(x)dx, \end{aligned} \right\} \quad 0 \leq x_0 \leq \ell,$$

and the inner products

$$(q_1, p_1)_1 = \int_0^{h_1} q_1(y)\overline{p_1(y)}dy, \quad (q_2, p_2)_2 = \int_0^\ell q_2(x)\overline{p_2(x)}dx.$$

K_{11} is a self-adjoint operator on $L_2(0, h_1)$, K_{22} is a self-adjoint operator on $L_2(0, \ell)$, K_{12} maps $L_2(0, \ell)$ into $L_2(0, h_1)$ and K_{21} maps $L_2(0, h_1)$ into $L_2(0, \ell)$. Indeed, $K_{21} = K_{12}^*$, where the asterisk denotes the adjoint, since $(K_{21}q_1, q_2)_2 = (q_1, K_{12}q_2)_1$ follows on using (3.22).

If we now write

$$\left. \begin{aligned} f_{1i} &= \psi_{i,0}(y), & 0 \leq y \leq h_i, \quad i = 1, 2, \\ f_{21}(x) &= 0, \quad f_{22}(x) = i \sin(k_2 x) \chi_{2,0}(h(x)), & 0 \leq x \leq \ell \end{aligned} \right\} \quad (3.25)$$

(noting that f_{22} is real-valued) then (3.15) and (3.21) can be re-cast as the operator equations

$$\left. \begin{aligned} K_{11}q_1 + K_{12}q_2 &= (A_1 + B_1)f_{11} + (A_2 + B_2)f_{12} & \text{in } L_2(0, h_1), \\ K_{21}q_1 + K_{22}q_2 &= (A_1 + B_1)f_{21} + (A_2 + B_2)f_{22} & \text{in } L_2(0, \ell). \end{aligned} \right\}$$

These can be reduced further to the equation

$$\mathbf{K}\mathbf{q} = (A_1 + B_1)\mathbf{f}_1 + (A_2 + B_2)\mathbf{f}_2 \quad (3.26)$$

in $L_2(0, h_1) \oplus L_2(0, \ell)$, where

$$\mathbf{K} = \begin{pmatrix} K_{11} & K_{12} \\ K_{21} & K_{22} \end{pmatrix}, \quad \mathbf{q} = \begin{pmatrix} q_1 \\ q_2 \end{pmatrix}, \quad \mathbf{f}_i = \begin{pmatrix} f_{1i} \\ f_{2i} \end{pmatrix}$$

and the composite inner product

$$\langle \mathbf{q}, \mathbf{p} \rangle = (q_1, p_1)_1 + (q_2, p_2)_2$$

is now appropriate, where $\mathbf{p} = (p_1, p_2)^T$. The operator matrix \mathbf{K} is self-adjoint on $L_2(0, h_1) \oplus L_2(0, \ell)$ since $\langle \mathbf{K}\mathbf{q}, \mathbf{p} \rangle = \langle \mathbf{q}, \mathbf{K}\mathbf{p} \rangle$.

The solution of (3.26) is given by

$$\mathbf{q} = (A_1 + B_1)\mathbf{q}^{(1)} + (A_2 + B_2)\mathbf{q}^{(2)}, \quad (3.27)$$

where

$$\mathbf{K}\mathbf{q}^{(i)} = \mathbf{f}_i, \quad i = 1, 2. \quad (3.28)$$

Now the equations (3.23) can be written as

$$B_1 = A_1 - \frac{i}{k_1 h_1} \langle \mathbf{q}, \mathbf{f}_1 \rangle, \quad B_2 = A_2 - \frac{i}{k_2 h_2} \langle \mathbf{q}, \mathbf{f}_2 \rangle,$$

and, if we use (3.27) in these expressions and rearrange the resulting equations into the form given in (2.9), we find that the scattering matrix is given by

$$\mathbf{S} = (\mathbf{D} + i\mathbf{Q})^{-1}(\mathbf{D} - i\mathbf{Q}) \quad (3.29)$$

in which

$$\mathbf{D} = \begin{pmatrix} k_1 h_1 & 0 \\ 0 & k_2 h_2 \end{pmatrix}, \quad \mathbf{Q} = \begin{pmatrix} \langle \mathbf{q}^{(1)}, \mathbf{f}_1 \rangle & \langle \mathbf{q}^{(2)}, \mathbf{f}_1 \rangle \\ \langle \mathbf{q}^{(1)}, \mathbf{f}_2 \rangle & \langle \mathbf{q}^{(2)}, \mathbf{f}_2 \rangle \end{pmatrix}. \quad (3.30)$$

The scattering matrix is therefore determined by the real quantities $\langle \mathbf{q}^{(i)}, \mathbf{f}_j \rangle$ for $i, j = 1, 2$. \mathbf{Q} is a symmetric matrix as $\langle \mathbf{q}^{(1)}, \mathbf{f}_2 \rangle = \langle \mathbf{q}^{(2)}, \mathbf{f}_1 \rangle$ follows from the self-adjointness of \mathbf{K} . This structure is familiar in other cases (see Porter 1995*b*) and the solution methods used there carry over directly to the present situation, as we shall show in § 5.

We remark that the identity $\mathbf{S}\overline{\mathbf{S}} = \mathbf{I}$ is a trivial consequence of (3.29), whatever the matrix \mathbf{Q} . This confirms an observation made in § 2 that the Kreisel (1949) relations are identities in any approximation to the solution (that is, to \mathbf{Q}) which incorporates the correct form of the far-field, as we have certainly done here.

We also note that, by virtue of the derivation, the problem of scattering by a

vertical step is embedded in our equations. Thus, if we discard contributions from C in (3.26) we obtain the single equation

$$K_{11}q_1 = (A_1 + B_1)\psi_{1,0} + (A_2 + B_2)\psi_{2,0} \quad \text{in } L_2(0, h_1)$$

appropriate to the vertical step case. Similar simplifications apply in (3.28) and the inner product $\langle \cdot, \cdot \rangle$ reduces to $(\cdot, \cdot)_1$. A corresponding reduction can be made to the semi-infinite reflection problem in which the undulating part of the bed remains but there is a solid boundary at $x = 0$ for $0 \leq y \leq h_1$. K_{22} is the only operator arising in this case. In the general problem we have formulated, the operators K_{12} and K_{21} serve to provide the interaction between these two limiting cases and the fact that one is the adjoint of the other is merely a consequence of the reciprocity in this interaction.

Before ending this section, it is worth noting that an alternative integral formulation of the scattering problem is possible. If we start out by defining the Green's functions G_- and G_+ in (3.1) and (3.5) as a difference between (as opposed to a sum of) pairs of Green's functions G_i , a coupled pair of integral equations based on the unknown potentials across the line $x = 0$, $0 \leq y \leq h_1$ and the curve $(x, y) \in C$ can be obtained. This alternative formulation does not make use of the Cauchy–Riemann relations used for transferring from normal to tangential derivatives, and, as a result, normal derivatives are explicit in the final formulation. This inevitably leads to a more complicated numerical solution, though there appear to be no inherent difficulties associated with this approach. Of particular interest is the structure of the solution obtained through this approach. A similar reduction to a coupled pair of integral equations can be made and the scattering matrix, \mathbf{S} , is now in terms of a matrix \mathbf{P} (say) which contains the inner products of a type similar to that defining \mathbf{Q} involving the functions related to unknown potentials instead of velocities. In particular, $\mathbf{P} = \mathbf{Q}^{-1}$, a reciprocal relation which evolves from so-called complementary formulations in a number of scattering and radiation problems described in Porter (1995) involving specific coordinate aligned geometries. In the problem being considered here, the boundaries are arbitrary.

The presence of an alternative formulation to a problem is always useful in confirming that the numerical results are correct as well as providing a gauge of their accuracy. Indeed, sometimes they may also provide upper and lower bounds on the solution (see, for example, Porter 1995). However, there is no evidence here to suggest that upper and lower bounds are present in this problem, and confirmation of the numerical results will be made by cross-checking with numerical results obtained from the formulation in the following section. Thus a full description of the alternative formulation is omitted from this paper. Finally, we note that in the problem of oblique wave incidence, where the Cauchy–Riemann equations are redundant and the formulation described in this section fails, a formulation based on unknown potentials is still possible.

4. Integral equations for a bed with a depression

With $h_3 > h_2$ (see figure 2) an additional region is needed to implement the solution method, as noted earlier, and this inevitably leads to additional complexity. However, we can make use of material developed in §2 and we can suppress details which mimic those described in the previous section.

The equations (3.3) and (3.4) remain unchanged in the revised circumstances. We can also deduce a suitable expression for $\phi(x_0, y_0)$ in $x_0 > \ell$ by a simple translation in (3.6), discarding the contribution from C and noting that the depth extends to $y = h_2$

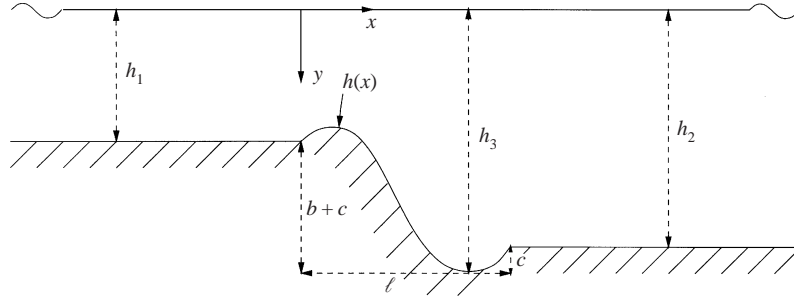


FIGURE 2. A bottom topography including a depression.

on $x = \ell$. We thus obtain

$$\phi(x_0, y_0) = 2A_2 \cos k_2(x_0 - \ell) \psi_{2,0}(y_0) - \int_0^{h_2} G_+(0, y | x_0 - \ell, y_0) \phi_x(\ell, y) dy, \quad \ell < x_0, \quad 0 < y_0 < h_2.$$

This short-cut has the effect of replacing the second element of (2.6) by

$$\phi(x, y) \sim \{A_2 e^{-ik_2(x-\ell)} + B_2 e^{ik_2(x-\ell)}\} \psi_{2,0}(y), \quad x \rightarrow \infty, \quad (4.1)$$

but we can continue to use the existing definition (2.9) for the scattering matrix \mathbf{S} despite this revision of the far-field behaviour. With this understanding,

$$B_2 = A_2 - \frac{i}{k_2 h_2} \int_0^{h_2} \psi_{2,0}(y) \phi_x(\ell, y) dy \quad (4.2)$$

follows from (3.9), and

$$\phi(\ell, y_0) = (A_2 + B_2) \psi_{2,0}(y_0) - \int_0^{h_2} \sum_{n=1}^{\infty} \frac{\psi_{2,n}(y) \psi_{2,n}(y_0)}{k_{2,n} h_2} \phi_x(\ell, y) dy, \quad 0 \leq y_0 \leq h_2, \quad (4.3)$$

from (3.13)

The bulk of the effort in this case is devoted to representing $\phi(x, y)$ appropriately in the region $0 < x < \ell$, $0 < y < h(x)$ between the two semi-infinite regions. To achieve this we use the Green's function $G = G_0$ satisfying (2.10) on $0 < x < \ell$, $0 < y < h_3$, (2.11) on $y = 0$ for $0 < x < \ell$, (2.12) on $y = h_3$ for $0 < x < \ell$ and $G_x = 0$ on $x = 0$ and $x = \ell$ for $0 < y < h_3$. By the method of images,

$$G_0(x, y | x_0, y_0) = \sum_{m=-\infty}^{\infty} \{G_3(2m\ell + x, y | x_0, y_0) + G_3(2m\ell - x, y | x_0, y_0)\},$$

in the notation of (2.15), and this simplifies to

$$G_0(x, y | x_0, y_0) = \sum_{n=0}^{\infty} \frac{\psi_{3,n}(y) \psi_{3,n}(y_0)}{2k_{3,n} h_3 \sinh(k_{3,n} \ell)} \{ \cosh k_{3,n}(\ell - |x - x_0|) + \cosh k_{3,n}(\ell - x - x_0) \}, \quad 0 < x_0 < \ell, \quad 0 < y_0 < h_3, \quad (4.4)$$

for $(x, y) \neq (x_0, y_0)$ and provided that $\sin(k_3 h_3) \neq 0$. Alternatively, the boundary-value problem for G_0 can be solved directly, by expanding in the set $\{\psi_{3,n}\}$. Applying (2.17)

over the domain of G_0 , we arrive at the equation

$$\begin{aligned} \phi(x_0, y_0) = & - \int_0^{h_1} G_0(0, y|x_0, y_0)\phi_x(0, y)dy + \int_0^{h_2} G_0(\ell, y|x_0, y_0)\phi_x(\ell, y)dy \\ & - \int_C \phi(x, y)\frac{\partial}{\partial n}G_0(x, y|x_0, y_0)ds, \quad 0 < x_0 < \ell, \quad 0 < y_0 < h(x). \end{aligned} \quad (4.5)$$

The way forward from this point is clear: we obtain two integral equations by matching (4.5) with (3.4) and (4.3) in turn and a further equation by applying the bed condition $\partial\phi(x_0, y_0)/\partial n_0 = 0$ on C , in (4.5). The unknown functions in these equations are q_1 and q_2 , defined in (3.14), together with the new quantity

$$q_3(y) = \phi_x(\ell, y), \quad 0 \leq y \leq h_2. \quad (4.6)$$

As in §3, we also have to interchange normal and tangential derivatives on C and we can expedite matters by setting out next all of the relationships needed for this purpose.

Using (2.20) with (4.4) we find that

$$\frac{\partial}{\partial n}G_0(x, y|0, y_0) = -\frac{\partial}{\partial s}F_0(\ell - x, y, y_0) \quad (4.7)$$

and

$$\frac{\partial}{\partial n}G_0(x, y|\ell, y_0) = \frac{\partial}{\partial s}F_0(x, y, y_0), \quad (4.8)$$

where

$$F_0(x, y, y_0) = \sum_{n=0}^{\infty} \frac{\chi_{3,n}(y)\psi_{3,n}(y_0) \sinh(k_{3,n}x)}{k_{3,n}h_3 \sinh(k_{3,n}\ell)}$$

is such that $F_0(0, y, y_0) = 0$ and (by using an expansion similar to (3.12)) $F_0(\ell, h_2, y_0) = 0$ for $0 \leq y < h_2$. We also use (4.7) and (4.8) with (x, y) and (x_0, y_0) interchanged. Further,

$$\frac{\partial^2}{\partial n_0 \partial n}G_0(x, y|x_0, y_0) = -\frac{\partial^2}{\partial s_0 \partial s}H_0(x, y|x_0, y_0), \quad (x, y) \neq (x_0, y_0),$$

where

$$H_0(x, y|x_0, y_0) = \sum_{n=0}^{\infty} \frac{\chi_{3,n}(y)\chi_{3,n}(y_0)}{2k_{3,n}h_3 \sinh(k_{3,n}\ell)} \{ \cosh k_{3,n}(\ell - |x - x_0|) - \cosh k_{3,n}(l - x - x_0) \}$$

and

$$H_0(0, y|x_0, y_0) = H_0(\ell, y|x_0, y_0) = 0.$$

We can now derive the integral equations, using the preceding formulae in integrals over C in the process. First, equating the versions of $\phi(0, y_0)$ given by (3.4) and (4.5) we have

$$\begin{aligned} \int_0^{h_1} m_{11}(y_0, y)q_1(y)dy + \int_0^{\ell} m_{12}(y_0, x)q_2(x)dx + \int_0^{h_2} m_{13}(y_0, y)q_3(y)dy \\ = (A_1 + B_1)\psi_{1,0}(y_0), \quad 0 \leq y_0 \leq h_1, \end{aligned} \quad (4.9)$$

where

$$m_{11}(y, y_0) = \sum_{n=1}^{\infty} \left\{ \frac{\psi_{1,n}(y_0)\psi_{1,n}(y)}{k_{1,n}h_1} + \frac{\psi_{3,n}(y_0)\psi_{3,n}(y)}{k_{3,n}h_3 \tanh(k_{3,n}\ell)} \right\} - \frac{\psi_{3,0}(y_0)\psi_{3,0}(y)}{k_3h_3 \tan(k_3\ell)}, \quad (4.10)$$

$$m_{12}(y_0, x) = \sum_{n=0}^{\infty} \frac{\chi_{3,n}(h(x))\psi_{3,n}(y_0) \sinh k_{3,n}(\ell - x)}{k_{3,n}h_3 \sinh(k_{3,n}\ell)}, \quad (4.11)$$

and

$$m_{13}(y_0, y) = - \sum_{n=0}^{\infty} \frac{\psi_{3,n}(y)\psi_{3,n}(y_0)}{k_{3,n}h_3 \sinh(k_{3,n}\ell)}. \quad (4.12)$$

Next, the condition $\partial\phi/\partial n_0 = 0$ on C used in (4.5) leads to

$$\begin{aligned} \int_0^{h_1} F_0(\ell - x_0, y_0, y)\phi_x(0, y)dy - \int_C H_0(x, y|x_0, y_0) \frac{\partial\phi(x, y)}{\partial s} ds \\ + \int_0^{h_2} F_0(x_0, y_0, y)\phi_x(\ell, y)dy = \text{constant}, \quad (x_0, y_0) \in C \end{aligned}$$

and the constant vanishes by letting $(x_0, y_0) \rightarrow (\ell, h_2)$. The resulting equation can be written in the form

$$\int_0^{h_1} m_{21}(x_0, y)q_1(y)dy + \int_0^{\ell} m_{22}(x_0, x)q_2(x)dx + \int_0^{h_2} m_{23}(x_0, y)q_3(y)dy = 0, \quad 0 \leq x_0 \leq \ell, \quad (4.13)$$

in which

$$m_{21}(x_0, y) = m_{12}(y, x_0), \quad (4.14)$$

$$m_{22}(x_0, x) = - \sum_{n=0}^{\infty} \frac{\chi_{3,n}(h(x))\chi_{3,n}(h(x_0))}{2k_{3,n}h_3 \sinh(k_{3,n}\ell)} \{ \cosh k_{3,n}(\ell - |x - x_0|) - \cosh k_{3,n}(\ell - x - x_0) \} \quad (4.15)$$

and

$$m_{23}(x_0, y) = \sum_{n=0}^{\infty} \frac{\chi_{3,n}(h(x_0))\psi_{3,n}(y) \sinh(k_{3,n}x_0)}{k_{3,n}h_3 \sinh(k_{3,n}\ell)}. \quad (4.16)$$

Finally, matching (4.3) with (4.5), evaluated at $x = \ell$, we obtain

$$\begin{aligned} \int_0^{h_1} m_{31}(y_0, y)q_1(y)dy + \int_0^{\ell} m_{32}(y_0, x)q_2(x)dx + \int_0^{h_2} m_{33}(y_0, y)q_3(y)dy \\ = (A_2 + B_2)\psi_{2,0}(y_0), \quad 0 \leq y_0 \leq h_2, \end{aligned} \quad (4.17)$$

the kernels in this case being given by

$$m_{31}(y_0, y) = m_{13}(y, y_0), \quad m_{32}(y_0, x) = m_{23}(x, y_0) \quad (4.18)$$

and

$$m_{33}(y_0, y) = \sum_{n=1}^{\infty} \left\{ \frac{\psi_{2,n}(y)\psi_{2,n}(y_0)}{k_{2,n}h_2} + \frac{\psi_{3,n}(y)\psi_{3,n}(y_0)}{k_{3,n}h_3 \tanh(k_{3,n}\ell)} \right\} - \frac{\psi_{3,0}(y)\psi_{3,0}(y_0)}{k_3h_3 \tan(k_3\ell)}. \quad (4.19)$$

The three coupled integral equations for this case are therefore (4.9), (4.13) and (4.17); we note that all of the kernels m_{ij} are real-valued. Some economy can be

achieved in defining the corresponding operators M_{ij} by writing I_1 , I_2 and I_3 to denote the intervals $[0, h_1]$, $[0, \ell]$ and $[0, h_2]$ respectively. Then

$$(M_{ij}q)(\xi) = \int_{I_j} m_{ij}(\xi, \eta)q(\eta)d\eta, \quad \xi \in I_i,$$

which maps $L_2(I_j)$ into $L_2(I_i)$. The property $m_{ij}(\xi, \eta) = m_{ji}(\eta, \xi)$ implies that $(M_{ij}q, p)_i = (q, M_{ij}p)_j$, showing that $M_{ij} = M_{ji}^*$ for $i, j = 1, 2, 3$. The inner product notation

$$(q, p)_i = \int_{I_i} q(\eta)\overline{p(\eta)}d\eta, \quad i = 1, 2, 3,$$

is a direct extension of that used in § 3.

If we now write $\mathbf{q} = (q_1, q_2, q_3)^T$, with $q_i \in L_2(I_i)$, the integral equation system consisting of (4.9), (4.13) and (4.17) can be represented by the single operator equation

$$\mathbf{M}\mathbf{q} = (A_1 + B_1)\mathbf{g}_1 + (A_2 + B_2)\mathbf{g}_2 \tag{4.20}$$

in $L_2(0, h_1) \oplus L_2(0, \ell) \oplus L_2(0, h_2)$, where

$$\mathbf{M} = \begin{pmatrix} M_{11} & M_{12} & M_{13} \\ M_{21} & M_{22} & M_{23} \\ M_{31} & M_{32} & M_{33} \end{pmatrix}, \quad \mathbf{g}_1 = \begin{pmatrix} \psi_{1,0} \\ 0 \\ 0 \end{pmatrix}, \quad \mathbf{g}_2 = \begin{pmatrix} 0 \\ 0 \\ \psi_{2,0} \end{pmatrix}.$$

Thus

$$\mathbf{q} = (A_1 + B_1)\mathbf{q}^{(1)} + (A_2 + B_2)\mathbf{q}^{(2)}$$

where

$$\mathbf{M}\mathbf{q}^{(i)} = \mathbf{g}_i, \quad i = 1, 2. \tag{4.21}$$

Moreover, in terms of the inner product

$$[\mathbf{q}, \mathbf{p}] = (q_1, p_1)_1 + (q_2, p_2)_2 + (q_3, p_3)_3$$

corresponding to (4.20), where $\mathbf{p} = (p_1, p_2, p_3)^T$ and $p_i \in L_2(I_i)$, (3.3) and (4.2) are

$$B_1 = A_1 - \frac{i}{k_1 h_1} [\mathbf{q}, \mathbf{g}_1], \quad B_2 = A_2 - \frac{i}{k_2 h_2} [\mathbf{q}, \mathbf{g}_2].$$

It follows, as in § 3, that the scattering matrix is given by (3.29) with \mathbf{D} defined as in (3.30) but with \mathbf{Q} replaced by

$$\mathbf{Q} = \begin{pmatrix} [\mathbf{q}^{(1)}, \mathbf{g}_1] & [\mathbf{q}^{(2)}, \mathbf{g}_1] \\ [\mathbf{q}^{(1)}, \mathbf{g}_2] & [\mathbf{q}^{(2)}, \mathbf{g}_2] \end{pmatrix}.$$

As $[\mathbf{M}\mathbf{q}, \mathbf{p}] = [\mathbf{q}, \mathbf{M}\mathbf{p}]$, the overall structure is thus the same as that obtained in the previous section, the only significant difference being the inevitable increase in the dimension of the operator matrix.

We note that the undulating part of the bed does not influence the far-field directly in this case, but only through q_1 and q_3 . The right-hand sides of (4.21) are therefore unaltered by changes in the bed shape $h(x)$. In particular, the integral equation system for the underlying rectangular geometry obtained by omitting all reference to the interval I_2 , is

$$\begin{pmatrix} M_{11} & M_{13} \\ M_{31} & M_{33} \end{pmatrix} \begin{pmatrix} q_1 \\ q_3 \end{pmatrix} = (A_1 + B_1) \begin{pmatrix} \psi_{1,0} \\ 0 \end{pmatrix} + (A_2 + B_2) \begin{pmatrix} 0 \\ \psi_{2,0} \end{pmatrix}, \tag{4.22}$$

which contains the same non-trivial forcing terms as (4.20). This reduced problem

corresponds to scattering by a rectangular trench of quiescent depth h_3 , set between the two semi-infinite horizontal bed sections. The operator M_{22} is associated with sloshing motions over the bed $y = h(x)$, with solid vertical boundaries at $x = 0$ and $x = \ell$.

5. Approximation and numerical method

Because both of the bed formations we are considering lead to the same type of operator problem, we need only examine that arising in §3 in any detail.

We therefore seek approximations to the real quantities

$$\mathbf{Q}_{ij} = \langle \mathbf{q}^{(i)}, \mathbf{f}_j \rangle, \quad i, j = 1, 2, \quad (5.1)$$

where

$$\mathbf{K} \mathbf{q}^{(i)} = \mathbf{f}_i, \quad i = 1, 2, \quad (5.2)$$

and \mathbf{K} is a self-adjoint operator on $\mathcal{H} = L_2(0, h_1) \oplus L_2(0, \ell)$, which is equipped with the inner product $\langle \cdot, \cdot \rangle$.

The functional $J_2 : \mathcal{H} \times \mathcal{H} \rightarrow \mathbf{C}$ defined by

$$J_2(\mathbf{p}^{(1)}, \mathbf{p}^{(2)}) = \langle \mathbf{p}^{(1)}, \mathbf{f}_2 \rangle + \langle \mathbf{f}_1, \mathbf{p}^{(2)} \rangle - \langle \mathbf{K} \mathbf{p}^{(1)}, \mathbf{p}^{(2)} \rangle \quad (5.3)$$

is easily seen to be stationary at $\mathbf{p}^{(i)} = \mathbf{q}^{(i)}$, $i = 1, 2$, and the stationary value is $J_2(\mathbf{q}^{(1)}, \mathbf{q}^{(2)}) = \mathbf{Q}_{12} = \mathbf{Q}_{21}$. The reduced functional $J_1(\mathbf{p}^{(i)}) : \mathcal{H} \rightarrow \mathbf{R}$, where

$$J_1(\mathbf{p}^{(i)}) = \langle \mathbf{p}^{(i)}, \mathbf{f}_i \rangle + \langle \mathbf{f}_i, \mathbf{p}^{(i)} \rangle - \langle \mathbf{K} \mathbf{p}^{(i)}, \mathbf{p}^{(i)} \rangle \quad (5.4)$$

is also stationary at $\mathbf{p}^{(i)} = \mathbf{q}^{(i)}$, for $i = 1, 2$, and $J_1(\mathbf{q}^{(i)}) = \mathbf{Q}_{ii}$ is the stationary value. We can therefore obtain estimates, $\tilde{\mathbf{Q}}_{ij}$ say, of \mathbf{Q}_{ij} by approximating $\mathbf{q}^{(i)}$ by $\tilde{\mathbf{q}}^{(i)} \in \mathcal{H}_{N+1}$, a chosen $(N + 1)$ -dimensional subspace of \mathcal{H} , and these will be second-order accurate in the sense that

$$|\mathbf{Q}_{ij} - \tilde{\mathbf{Q}}_{ij}| = O(\|\mathbf{q}^{(i)} - \tilde{\mathbf{q}}^{(i)}\| \|\mathbf{q}^{(j)} - \tilde{\mathbf{q}}^{(j)}\|).$$

Suppose then that \mathcal{H}_{N+1} is spanned by the given functions $\mathbf{p}_0, \dots, \mathbf{p}_N$, and hence that

$$\tilde{\mathbf{q}}^{(i)} = \sum_{n=0}^N c_n^{(i)} \mathbf{p}_n, \quad i = 1, 2. \quad (5.5)$$

Then the stationary points, $\tilde{\mathbf{q}}^{(i)} \approx \mathbf{q}^{(i)}$ of both $J_1(\tilde{\mathbf{q}}^{(i)})$ and $J_2(\tilde{\mathbf{q}}^{(1)}, \tilde{\mathbf{q}}^{(2)})$ are given by solving

$$\langle \mathbf{K} \tilde{\mathbf{q}}^{(i)} - \mathbf{f}_i, \mathbf{p}_m \rangle = 0, \quad m = 0, \dots, N, \quad (5.6)$$

for $c_0^{(i)}, \dots, c_N^{(i)}$, with $i = 1, 2$. The equations (5.5) and (5.6) also characterize Galerkin's method in the present case. Combining them gives the system of equations which determines the coefficients in (5.5) explicitly, in the form

$$\sum_{n=0}^N c_n^{(i)} \langle \mathbf{K} \mathbf{p}_n, \mathbf{p}_m \rangle = \langle \mathbf{f}_i, \mathbf{p}_m \rangle, \quad m = 0, \dots, N, \quad (5.7)$$

for $i = 1, 2$. The approximations to \mathbf{Q}_{ij} are given by

$$\tilde{\mathbf{Q}}_{ij} = \sum_{n=0}^N c_n^{(i)} \langle \mathbf{p}_n, \mathbf{f}_j \rangle, \quad i, j = 1, 2, \quad (5.8)$$

and it is automatic that $\tilde{\mathbf{Q}}_{12} = \tilde{\mathbf{Q}}_{21}$.

This approximation method has been used in the scalar case by Porter & Evans (1995) and in a similar vector case by Porter (1995) where it gives high accuracy for relatively small values of N provided that the subspace is judiciously chosen, something that will be addressed later.

The vector notation introduced above has been used for compactness. In order to present the implementation of the approximation method, it is clearer to revert to the coupled system and consider separately equations relating to the components associated with $q_1(y)$ and $q_2(x)$ and defined on the intervals $0 \leq y \leq h_1$ and $0 \leq x \leq \ell$. Thus, instead of (5.5) we write

$$\left. \begin{aligned} \tilde{q}_1^{(i)}(y) &= \sum_{n=0}^{N_1} c_n^{(1i)} u_n(y), & 0 < y < h_1 \\ \tilde{q}_2^{(i)}(x) &= \sum_{n=0}^{N_2} c_n^{(2i)} v_n(x), & 0 < x < \ell. \end{aligned} \right\} \quad i = 1, 2,$$

where the choice of test functions $\{u_n\}$, $n = 0, \dots, N_1$ and $\{v_n\}$, $n = 0, \dots, N_2$ remain arbitrary at this juncture and will be considered later, whilst the coefficients $c_n^{(1i)}$, $n = 0, \dots, N_1$ and $c_n^{(2i)}$, $n = 0, \dots, N_2$ for $i = 1, 2$ are to be determined.

The Galerkin approximation (5.7) now takes the form of a coupled system of equations for the unknown coefficients given by

$$\left. \begin{aligned} \sum_{n=0}^{N_1} c_n^{(1i)} K_{mn}^{(11)} + \sum_{n=0}^{N_2} c_n^{(2i)} K_{mn}^{(12)} &= F_{m0}^{(1i)}, & m = 0, \dots, N_1 \\ \sum_{n=0}^{N_1} c_n^{(1i)} K_{mn}^{(21)} + \sum_{n=0}^{N_2} c_n^{(2i)} K_{mn}^{(22)} &= F_{m0}^{(2i)}, & m = 0, \dots, N_2 \end{aligned} \right\} \quad i = 1, 2, \quad (5.9)$$

and from (5.8)

$$\tilde{\mathbf{q}}_{ij} = \sum_{n=0}^{N_1} c_n^{(1i)} F_{n0}^{(1j)} + \sum_{n=0}^{N_2} c_n^{(2i)} F_{n0}^{(2j)}, \quad i, j = 1, 2.$$

The four matrix elements of the block matrix system are given as follows:

$$K_{mn}^{(11)} = (K_{11} u_n, u_m)_1 = \sum_{r=1}^{\infty} \left\{ \frac{F_{nr}^{(11)} F_{mr}^{(11)}}{k_{1,r} h_1} + \frac{F_{nr}^{(12)} F_{mr}^{(12)}}{k_{2,r} h_2} \right\}, \quad m, n = 0, \dots, N_1,$$

$$K_{mn}^{(12)} = (K_{12} v_n, u_m)_1 = \frac{b_n F_{m0}^{(12)}}{k_2 h_2} + \sum_{r=1}^{\infty} \frac{F_{nr}^{(22)} F_{mr}^{(12)}}{k_{2,r} h_2}, \quad m = 0, \dots, N_1, \quad n = 0, \dots, N_2,$$

$$K_{mn}^{(21)} = K_{nm}^{(12)}, \quad m = 0, \dots, N_2, \quad n = 0, \dots, N_1,$$

$$K_{mn}^{(22)} = (K_{22} v_n, v_m)_2 = -w_{mn} + \frac{a_n b_m + a_m b_n}{2k_2 h_2} - e_{mn} + \sum_{r=1}^{\infty} \frac{F_{nr}^{(22)} F_{mr}^{(22)}}{2k_{2,r} h_2},$$

$m, n = 0, \dots, N_2,$

as a consequence of (3.16), (3.17), (3.22) and (3.23) where we have introduced the

notation

$$F_{nr}^{(1i)} = (u_n, \psi_{i,r})_1, \quad r = 0, 1, 2, \dots, \quad n = 0, 1, \dots, N_1, \quad i = 1, 2, \quad (5.10)$$

$$F_{nr}^{(22)} = \int_0^\ell \chi_{2,r}(h(x)) e^{-k_2 r x} v_n(x) dx, \quad r = 1, 2, \dots, \quad n = 0, 1, \dots, N_2 \quad (5.11)$$

with $F_{n0}^{(21)} = (v_n, f_{21})_2 = 0$, $F_{n0}^{(22)} = (v_n, f_{22})_2 \equiv a_n$ and

$$a_n = \int_0^\ell i \chi_{2,0}(h(x)) \sin(k_2 x) v_n(x) dx, \quad n = 0, 1, \dots, N_2, \quad (5.12)$$

$$b_n = \int_0^\ell i \chi_{2,0}(h(x)) \cos(k_2 x) v_n(x) dx, \quad n = 0, 1, \dots, N_2. \quad (5.13)$$

Lastly, we have written

$$w_{mn} = \frac{1}{2k_2 h_2} \int_0^\ell i \chi_{2,0}(h(x_0)) v_m(x_0) \int_0^\ell i \chi_{2,0}(h(x)) \sin(k_2 |x - x_0|) v_n(x) dx dx_0, \quad (5.14)$$

and

$$e_{mn} = \sum_{r=1}^{\infty} \frac{1}{2k_{2,r} h_2} \int_0^\ell \chi_{2,r}(h(x_0)) v_m(x_0) \int_0^\ell \chi_{2,r}(h(x)) e^{-k_{2,r} |x - x_0|} v_n(x) dx dx_0, \quad (5.15)$$

both for $m, n = 0, \dots, N_2$. Before continuing to the choice of the test functions, we make some remarks concerning the terms defined in (5.11)–(5.15) above. No further analytic progress can be made with those integrals containing the arbitrary topography $h(x)$ and these need to be computed numerically. This does not pose any problems for the terms $F_{nr}^{(22)}$, a_n , b_n and w_{mn} . The integral defining $F_{nr}^{(22)}$ involves the factor $\chi_{2,r}(h(x))$ which becomes increasingly oscillatory as r increases, though this is suppressed by the exponential factor allowing efficient and accurate numerical approximation of the integral. The term w_{mn} having an inseparable kernel requires numerical evaluation of a double integral although the integrand is well-behaved and the computation is again straightforward. In fact the only term which poses difficulties computationally is e_{mn} . In its present form e_{mn} is not suitable for computation, requiring the summation of a large number of terms (typically of the order of 500), each a double integral involving an increasingly oscillatory and inseparable integrand. Instead, the summation is taken inside both integrals such that only one double integration is present, but this switch is done at the expense of introducing a logarithmic singularity into the resulting kernel. Appendix A describes how this difficulty is overcome and we eventually write

$$e_{mn} = e_{mn}^{(1)} + e_{mn}^{(2)} + e_{mn}^{(3)}$$

where $e_{mn}^{(i)}$, $i = 1, 2, 3$ are given in the Appendix.

The choice of the set of test functions $\{u_n\}$ and $\{v_n\}$ can have a significant impact on the success of the numerical scheme. We first note that by choosing the functions to be real-valued, the matrix in (5.7) is real and symmetric and the right-hand-side terms are all real.

We are seeking good approximations to the quantities $q_1(y)$ and $q_2(x)$, being related to the horizontal fluid velocity across $x = 0$, $0 \leq y \leq h_1$ and the tangential fluid velocity along $y = h(x)$, $0 \leq x \leq \ell$ respectively. It is desirable to incorporate the physical behaviour of the fluid flow into our approximations and this can be done by examining the behaviour of $q_1(y)$ and $q_2(x)$ near the ends of $[0, h_1]$ and $[0, \ell]$,

respectively. Thus, a local analysis of solutions of (2.2) in the neighbourhood of $(0, h_1)$ and (ℓ, h_2) , and use of (2.3) and (2.13), shows that

$$q_1'(0) + Kq_1(0) = 0, \quad (5.16)$$

$$q_1(y) \sim (h_1 - y)^{\gamma_1}, \quad y \sim h_1, \quad (5.17)$$

$$q_2(x) \sim \{x^2 + (h(x) - h_1)^2\}^{\gamma_1/2}, \quad x \sim 0, \quad (5.18)$$

$$q_2(x) \sim \{(x - \ell)^2 + (h_2 - h(x))^2\}^{\gamma_2/2}, \quad x \sim \ell, \quad (5.19)$$

where $\gamma_i = \beta_i/(\pi - \beta_i)$, $-\frac{1}{2}\pi < \beta_i < \frac{1}{2}\pi$ ($i = 1, 2$), $\tan \beta_1 = h'(0)$ and $\tan \beta_2 = -h'(\ell)$.

In the particular case when the sloping part of the bed joins the constant depths h_1 and h_2 at $x = 0$ and $x = \ell$ smoothly, a natural choice of test functions satisfying the conditions (5.16)–(5.19) above is

$$u_n(y) = h_1^{-1} \psi_{1,n}(y), \quad n = 0, \dots, N_1, \quad 0 \leq y \leq h_1 \quad (5.20)$$

and

$$v_n(x) = \ell^{-1} \cos \frac{n\pi x}{\ell}, \quad n = 0, \dots, N_2, \quad 0 \leq x \leq \ell. \quad (5.21)$$

Use of (5.20) in (5.10) results simply in

$$F_{nr}^{(11)} = \delta_{nr}$$

(where δ_{nr} is the Kronecker delta) and

$$F_{nr}^{(12)} = -\frac{N_{2,r}^{-1/2} N_{1,n}^{-1/2} k_{2,r} \sin k_{2,r}(h_2 - h_1)}{(k_{2,r}^2 - k_{1,n}^2)h_1}.$$

The cases when either $n = 0$ or $r = 0$ or both $n = r = 0$ are recovered using $k_{i,0} = -ik_i$ ($i = 1, 2$).

In the general case, in which the undulating part of the bed does not join the constant depths h_1 and h_2 smoothly, we aim to use functions which satisfy the conditions (5.15)–(5.19) whilst providing as much simplification to the final expressions as possible. From (5.11)

$$\begin{aligned} F_{nr}^{(1i)} &= \int_0^{h_1} \psi_{i,r}(y) u_n(y) dy, \\ &= N_{i,r}^{-1/2} \int_0^{h_1} u_n(y) \cos k_{i,r}(h_i - y) dy, \\ &= N_{i,r}^{-1/2} \cos k_{i,r} h_i \int_0^{h_1} \hat{u}_n(y) \cos k_{i,r} y dy, \end{aligned} \quad (5.22)$$

where we have introduced the reduced function

$$\hat{u}_n(y) = u_n(y) - K \int_y^{h_1} u_n(t) dt,$$

which is such that the condition (5.16) translates to the condition

$$\hat{u}_n'(0) = 0, \quad (5.23)$$

on $\hat{u}_n(y)$. We define

$$\hat{u}_n(y) = \frac{(-1)^n 2^{\gamma_1+1/2} (2n)! \Gamma(\gamma_1 + \frac{1}{2})}{\pi h_1 \Gamma(2n + 2\gamma_1 + 1)} (1 - (y/h_1)^2)^{\gamma_1} C_{2n}^{\gamma_1+1/2}(y/h_1), \quad 0 \leq y \leq h_1, \quad (5.24)$$

where $C_n^v(x)$ is the orthogonal Gegenbauer polynomial. Notice that $C_{2n}^{\gamma_1+1/2}(x)$ is an even function of x and ensures that the reduced free-surface condition (5.23) is satisfied. Also notice that the correct corner behaviour at $y \sim h_1$ is incorporated into the definition of $\hat{u}_n(y)$, being the natural weighting function associated with the Gegenbauer polynomial. Inserting (5.24) into (5.22) and using the result (Gradshteyn & Ryzhik 1981, §7.324(2)) gives

$$F_{nr}^{(1i)} = N_{i,r}^{-1/2} \frac{\cos k_{i,r} h_i}{(k_{i,r} h_1)^{\gamma_1+1/2}} J_{2n+\gamma_1+1/2}(k_{i,r} h_1),$$

whilst,

$$F_{n0}^{(1i)} = (-1)^n N_{i,0}^{-1/2} \frac{\cosh k_i h_i}{(k_i h_1)^{\gamma_1+1/2}} I_{2n+\gamma_1+1/2}(k_i h_1),$$

where $J_\mu(x)$, $I_\mu(x)$ are first and second kind Bessel functions. A similar choice of functions and implementation has been used with success in the case of scattering by a vertical step by Porter (1995).

The choice of trial function for the undulating part of the bed is determined by the behaviour of the tangential velocity at the ends of the interval $[0, \ell]$ given by (5.18), (5.19). Although we cannot integrate expressions involving $v_n(x)$ explicitly due to the general nature of $h(x)$, as we have done for the integrals involving $u_n(y)$ above, the choice of $v_n(x)$ is motivated in the same way.

Thus therefore seek a set of polynomials which are orthogonal with respect to the weighting $(\ell - x)^{\gamma_2} x^{\gamma_1}$, reflecting the behaviour local to the points $x = 0$, $x = \ell$. This gives us

$$v_n(x) = \ell^{-1} (1 - x/\ell)^{\gamma_2} (x/\ell)^{\gamma_1} P_n^{(\gamma_2, \gamma_1)}(2x/\ell - 1), \quad 0 \leq x \leq \ell, \quad (5.25)$$

where $P_n^{(\alpha, \beta)}(x)$, $x \in [-1, 1]$ is the orthogonal Jacobi polynomial. The first two terms are simply

$$P_0^{(\alpha, \beta)}(x) = 1, \quad P_1^{(\alpha, \beta)}(x) = \frac{1}{2}((1 + \beta)(1 + x) - (1 + \alpha)(1 - x)), \quad -1 \leq x \leq 1,$$

and $P_n^{(\alpha, \beta)}(x)$, $n \geq 2$ follow from a recurrence relation (see Gradshteyn & Ryzhik 1981, §8.961(2)). When the section of varying topography joins the depths h_1 and h_2 smoothly, $\gamma_i = 0$, $i = 1, 2$, and the Jacobi polynomials reduce to Legendre polynomials. If only one of the two joins is a smooth one, the polynomials reduce to Gegenbauer polynomials, of which the even members have already been used in the approximation to $q_1(y)$.

The numerical method for the case when the bed undergoes a depression to a depth h_3 below the depth h_2 is similar to the case described above, the only significant difference being, of course, that there is another unknown function, $q_2(y)$, to be approximated relating to the horizontal fluid velocity across the boundary $x = \ell$, $0 \leq y \leq h_2$ (note in this case that $q_3(x)$ now represents the tangential velocity). The approximation of the function $q_2(y)$ follows closely the implementation of the approximation of $q_1(y)$ described in the case above. The only terms requiring particular attention in this case are the matrix elements associated with the kernel $m_{22}(x, x_0)$ defined in (4.15), which involve an inseparable term having the same asymptotic behaviour as the inseparable term in the kernel $k_{22}(x, x_0)$ given by (3.23). Thus the computation of these matrix elements is treated in precisely the manner outlined previously in this section and in the Appendix. As a final detail, in order to compute some of the terms in the depressed bed case, it is best to decompose the hyperbolic

N_1	N_2	$\tilde{\mathbf{Q}}_{11}$	$\tilde{\mathbf{Q}}_{12}$	$\tilde{\mathbf{Q}}_{22}$	$ R_2 $	$ \tilde{T}_2 $
0	0	1.060470	1.154720	1.252775	0.301564	1.368557
1	1	1.055371	1.147871	1.243602	0.302739	1.368023
2	2	1.055181	1.147616	1.243261	0.302782	1.368003
3	3	1.055179	1.147613	1.243255	0.302783	1.368003
4	4	1.055179	1.147613	1.243255	0.302782	1.368003

TABLE 1. Convergence of numerical method with truncation sizes N_1 and N_2 for a plane sloping profile, $\hat{h}(x) = 1 - x$, $h_1/h_2 = \frac{1}{4}$, $\ell/b = 1$.

terms such as $\sinh k_{3,n}\ell$ into $2 \sinh \frac{1}{2}k_{3,n}\ell \cosh \frac{1}{2}k_{3,n}\ell$ and write, for example, $\sinh k_{3,n}(\ell - x)$ as $[\sinh k_{3,n}(\frac{1}{2}\ell - x) \cosh \frac{1}{2}k_{3,n}\ell + \cosh k_{3,n}(\frac{1}{2}\ell - x) \sinh \frac{1}{2}k_{3,n}\ell]$.

6. Results

In the examples below, we non-dimensionalize the bed function using the transformation

$$\hat{h}(x) = (h_2 - h(\ell x))/b, \quad 0 \leq x \leq 1 \quad (b = h_2 - h_1) \tag{6.1}$$

such that $\hat{h}(0) = 1$, $\hat{h}(1) = 0$ in the case of a bed with no depression.

Our first task is to assess the accuracy of the approach that has been adopted in this paper. We reiterate that the Kreisel (1949) relations are satisfied automatically by virtue of the form of the scattering matrix \mathbf{S} in (3.29) *whatever* the approximation to the unknown functions.

Attention is focused on the case of a bed without depression with the understanding that similar results follow in the case of a bed with depression. There are two truncation parameters N_1 and N_2 associated with the size of the trial space used for approximating the functions $q_1(y)$ and $q_2(x)$. In addition to these parameters there are some other numerical issues that must first be discussed. In order to claim a certain number of decimal places accuracy in the reflection and transmission coefficients, it is essential that the various block matrix elements $K_{mn}^{(ij)}$ are first computed to at least the same degree of accuracy. Inaccuracies in the calculation of these block matrix elements arises from two sources. First, the infinite sums that are involved in the definition of all the elements $K_{mn}^{(ij)}$ require truncation to a size N_r , say. We choose a value of $N_r = 2000$ for all the results presented in this paper. Note however, that in the computation of $e_{mn}^{(1)}$ in (A 2), it is sufficient to choose $N_r = \min \{2000, -h_2 \ln(\epsilon)/\pi|x - x_0|\}$ where ϵ is the tolerance, chosen here to be 10^{-8} . Secondly, integrals are approximated using a 10-point composite Gauss–Legendre rule with 40 subintervals, the exception being in the calculation of the terms $e_{mn}^{(2)}$ for which 200 subintervals are used to resolve the difficulty with the logarithmic singularity at the point $x = x_0 = \ell$ (see Appendix). However, $e_{mn}^{(2)}$ is independent of wave frequency and needs to be computed just once for each geometry. This particular choice of quadrature and value of N_r is sufficient to be able to compute the matrix elements to an accuracy of seven decimal places and to be able to claim six decimal place accuracy in the computed values of $\tilde{\mathbf{Q}}_{ij}$, $i, j = 1, 2$ and hence in R_i and T_i , $i = 1, 2$, as demonstrated in the tables below. In the figures presented in this paper, the number of subintervals is reduced from 40 to 20 which in turn reduces the accuracy of R_i and T_i ($i = 1, 2$) to five decimal places but increases the computational speed.

Table 1 shows the convergence of elements of the matrix $\tilde{\mathbf{Q}}$ in addition to the

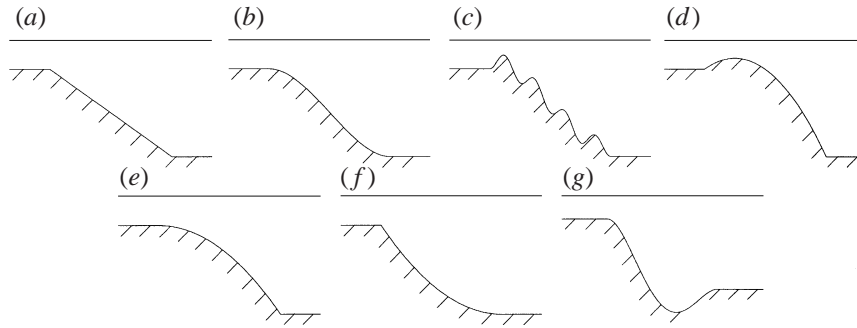


FIGURE 3. A set of bed profiles used in the results. In all cases, $h_1/h_2 = \frac{1}{4}$, $\ell/b = 1$, $c/b = \frac{1}{3}$.

modulus of the reflection and transmission coefficients $|R_1| = |R_2|$ and $|\tilde{T}_2|$ as N_1 and N_2 are increased in the case of a plane slope, defined by

$$\hat{h}(x) = 1 - x, \quad (6.2)$$

joining the depth h_1 to h_2 (see figure 3b), with $h_1/h_2 = \frac{1}{4}$, $\ell/b = 1$, such that the gradient of the slope is 45° , and with $k_2 h_2 = \frac{1}{2}$. Limited numerical results have been produced for this problem by Booij (1983) using a finite element method to compare with his results from the mild-slope equation. However, no results were tabulated. It can be seen from table 1 that six-figure accuracy has been achieved in $\tilde{\mathbf{Q}}$ with just four terms in the approximation, whilst just two terms is sufficient to gain three-figure accuracy.

The accuracy of the results shown in table 1 has been verified independently by comparing with the results from the formulation for a bed with depression using the same function in (6.2) and a general choice of $h_3 > h_2$. A similar rate of convergence is exhibited in the results from this independent approach, although the speed of computation is reduced for increased values of h_3 .

Finally, we present in table 2 the convergence of $\tilde{\mathbf{Q}}_{ij}$ and $|R|$ and $|T|$ with N_1 and N_2 when the general expansion functions $u_n(y)$ and $v_n(x)$ defined by (5.24) and (5.25) are replaced by the functions appropriate to a smoothly-joining topography in (5.20) and (5.21) to monitor their performance when applied in the case of a geometry with a non-smooth bed shape. Despite not having explicitly incorporated the singularity in the velocity at the corner $(0, h_1)$ into the trial functions, the approximations to the various quantities are nevertheless impressive though not as good as those in table 1, as expected. Furthermore, convergence towards the exact solution can be very slow and in this case, for example, with $N_1 = N_2 = 20$, the value of $|R_2|$ has only converged to a value of 0.302793. Even so, the level of accuracy that has been achieved with this crude choice of trial function demonstrates the power of the variational method when used to approximate solutions to integral equations.

The results given in table 1 are typical of bed shapes where there is limited variation in the slope along the length of the undulating part of the bed and for wavelengths that exceed the length of the bed. Care must be taken in the choice of N_2 for two reasons. Clearly, the tangential velocity on the sloping bed will, to some extent, adopt the signature of the free-surface displacement and will therefore require a trial space large enough to model this oscillatory behaviour in the function $q_2(x)$. For example, in the calculation of $|R_2|$ in the case of a plane slope defined by (6.1) with $\ell/b = 8$, $k_2 h_2 = 4$ (corresponding to $\ell \approx 4$ wavelengths) used in producing results in figure 5,

N_1	N_2	\tilde{Q}_{11}	\tilde{Q}_{12}	\tilde{Q}_{22}	$ R_2 $	$ \tilde{T}_2 $
0	0	1.082319	1.177810	1.276852	0.300768	1.368918
1	1	1.055734	1.148677	1.244950	0.302416	1.368170
2	2	1.055749	1.148334	1.244152	0.302675	1.368052
3	3	1.054867	1.147358	1.243073	0.302738	1.368023
4	4	1.054920	1.147373	1.243040	0.302767	1.368010

TABLE 2. Convergence of numerical method with same parameters used to produce table 1, but with the expansion functions $u_n(y)$ and $v_n(x)$ defined in (5.20) and (5.21) respectively.

N_1	N_2	\tilde{Q}_{11}	\tilde{Q}_{12}	\tilde{Q}_{22}	$ R_2 $	$ \tilde{T}_2 $	$ R_2 ^{(*)}$
0	0	0.724442	0.817679	0.914840	0.303800	1.367538	0.303761
1	1	0.571141	0.648120	0.727342	0.333488	1.353210	0.331988
2	2	0.542264	0.613808	0.686592	0.344262	1.347640	0.342892
3	3	0.540882	0.611850	0.683843	0.345149	1.347173	0.347186
4	4	0.540276	0.611135	0.682999	0.345384	1.347049	0.347915
5	5	0.527989	0.597571	0.668024	0.349130	1.345058	0.347889
6	6	0.514292	0.583164	0.652871	0.352619	1.343181	0.348305
7	7	0.509200	0.577432	0.646419	0.354466	1.342179	0.351389
8	8	0.508958	0.577232	0.646253	0.354454	1.342186	0.355065
9	9	0.502775	0.571280	0.640525	0.355390	1.341676	0.355989
10	10	0.494495	0.563403	0.633031	0.356575	1.341028	0.356153
	\vdots	\vdots	\vdots	\vdots	\vdots	\vdots	\vdots
10	20	0.491965	0.561422	0.631380	0.356246	1.341208	0.356245

TABLE 3. Convergence of numerical method with truncation sizes N_1 and N_2 for $h_1/h_2 = \frac{1}{4}$, $\ell/b = 1$, $k_2h_2 = \frac{1}{2}$ and for $\hat{h}(x)$ in (6.4). The column $|R_2|^{(*)}$ is the reflection coefficient obtained by substituting the expansion functions (5.20) and (5.21).

values of $N_1 = 2$, $N_2 = 12$ are required to obtain the desired accuracy. Failure to use a large enough value of N_2 may lead to misleading results. Note, however, that for such large values of $k_2\ell$, there is often very little reflection.

For similar reasons, the truncation parameter N_2 must also be increased when the bed shape becomes more complex in order to accurately model the increased variations in $q_2(x)$ along it. A particularly severe test of the method is illustrated in table 3 for a slope profile is given by the function

$$\hat{h}(x) = 1 + 2x^3 - 3x^2 + A_h(1 - \cos(2s\pi x)) \tag{6.3}$$

with $A_h = \frac{1}{10}$, $s = 4$ and $h_1/h_2 = \frac{1}{4}$, ℓ/b (as illustrated in figure 3c) and $k_2h_2 = \frac{1}{2}$. As expected, the rate of convergence is not as good for this highly oscillatory bed shape. Nevertheless, with $N_1 = N_2 = 10$, the results are correct to three decimal places compared with the six decimal place accuracy that has been obtained for $N_1 = 10$, $N_2 = 20$. Also shown in table 3 are the values of $|R|$ computed using the expansion functions $u_n(y)$ and $v_n(x)$ defined in (5.20) and (5.21) for smoothly joining topography, which we are considering in this case. As we would expect, the rate of convergence and accuracy of the results computed using these functions in this case are comparable with the results obtained using the more general functions.

Further results have been obtained for numerous bed shapes but only a small sample of these can, of course, be presented here. We continue by presenting some

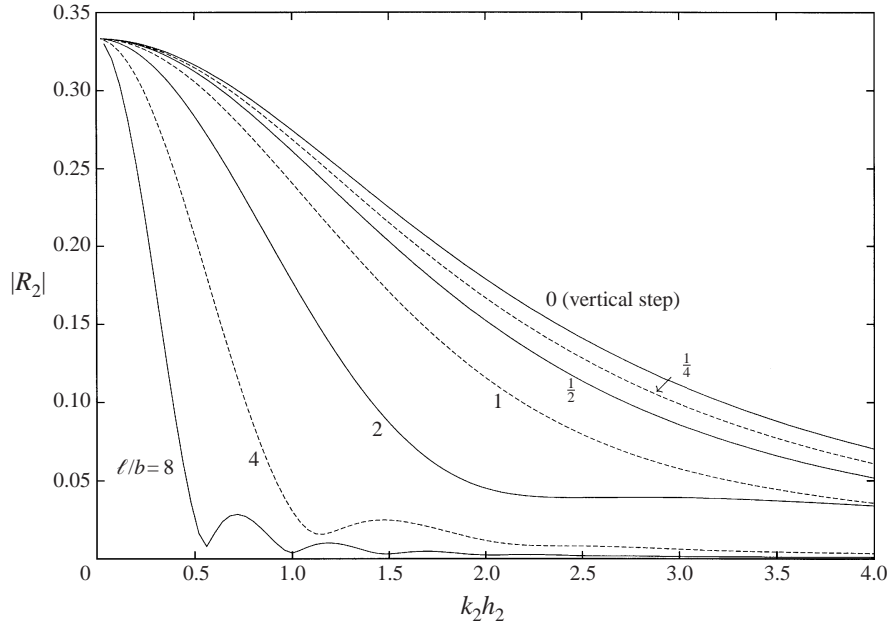


FIGURE 4. Reflection coefficient, $|R_2|$, against wavenumber k_2h_2 for the plane slope profile $\hat{h}(x) = 1 + 2x^3 - 3x^2$, $h_1/h_2 = \frac{1}{4}$ with various values of ℓ/b (shown against curves).

curves showing the variation of reflection coefficient with frequency for a selection of topographies.

In the long-wave limit, or as $\omega \rightarrow 0$, Lamb (1932, §176) gives the result $|R_i| \rightarrow (1 - \sqrt{h_1/h_2})/(1 + \sqrt{h_1/h_2})$, $i = 1, 2$, based on shallow water theory, stating that the reflection depends only on the constant depths at either infinity. Moreover as $\omega \rightarrow \infty$ $|R_i| \rightarrow 0$, $i = 1, 2$, though it is not clear how this limit is approached. Thus we are most interested in understanding the effect of the topography on wave reflection in the region $k_i h_i = O(1)$, $i = 1, 2$.

A bed without depression

In figure 4, we show the effect of the length of the slope on the reflection coefficient in the case of a smoothly varying bed profile, given by

$$\hat{h}(x) = 1 + 2x^3 - 3x^2 \quad (6.4)$$

for a depth ratio of $h_1/h_2 = \frac{1}{4}$ and for various bed lengths, $\ell/b = \frac{1}{2}, 1, 2, 4, 8$. Also shown in figure 4 is a curve of reflection against non-dimensional wavenumber k_2h_2 in the case of a vertical step (see Porter 1995). As expected, most reflection occurs in the case of a vertical step, decreasing as the gradient of the slope is reduced.

A similar set of results is shown in figure 5 in the case of a plane slope given by (6.2) with $h_1/h_2 = \frac{1}{4}$ again for $\ell/b = \frac{1}{2}, 1, 2, 4, 8$.

Another simply defined bed profile is given by

$$\hat{h}(x) = 1 - \alpha x^2 + (\alpha - 1)x \quad (6.5)$$

which provides a range of different bed shapes. If $\alpha = 0$, we recover the plane slope from the depth h_1 to h_2 described by equation (6.2). When $\alpha = 1$, the quadratic bed shape joins the level h_1 smoothly. For $\alpha > 1$, there is a protrusion above the level h_1

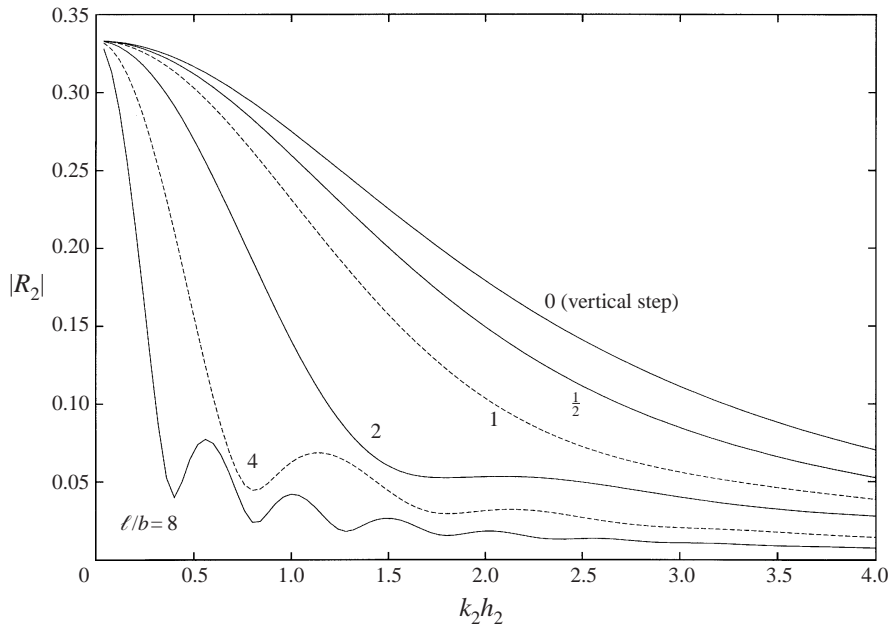


FIGURE 5. Reflection coefficient, $|R_2|$, against wavenumber k_2h_2 for the plane slope profile $\hat{h}(x) = 1 - x$, $h_1/h_2 = \frac{1}{4}$ with various values of ℓ/b (shown against curves).

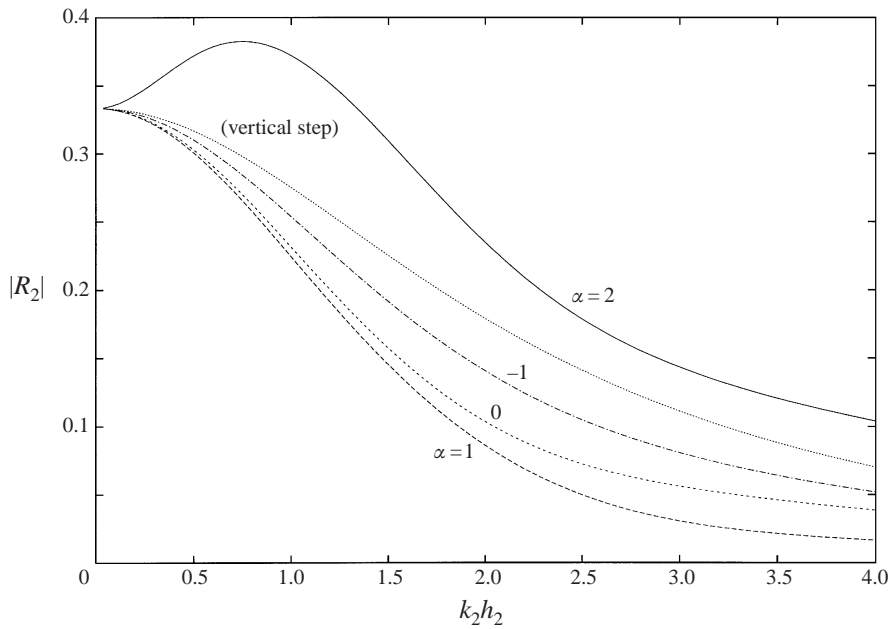


FIGURE 6. Reflection coefficient, $|R_2|$, against wavenumber k_2h_2 for the slope profiles given by $\hat{h}(x) = 1 - \alpha x^2 + (\alpha - 1)x$ for different values of α for $h_1/h_2 = \frac{1}{4}$, $\ell/b = 1$.

resulting in a minimum depth of $h_1 - (h_2 - h_1)(\alpha - 1)^2/4\alpha$ at a value of $x = (\alpha - 1)/2\alpha$. For $-1 \leq \alpha < 0$, the bed is concave. For $\alpha < -1$, we enter the regime of a depression below the depth h_2 which is considered in the next subsection.

From figure 6 it can be seen that with $\alpha = 2$, corresponding to the topography

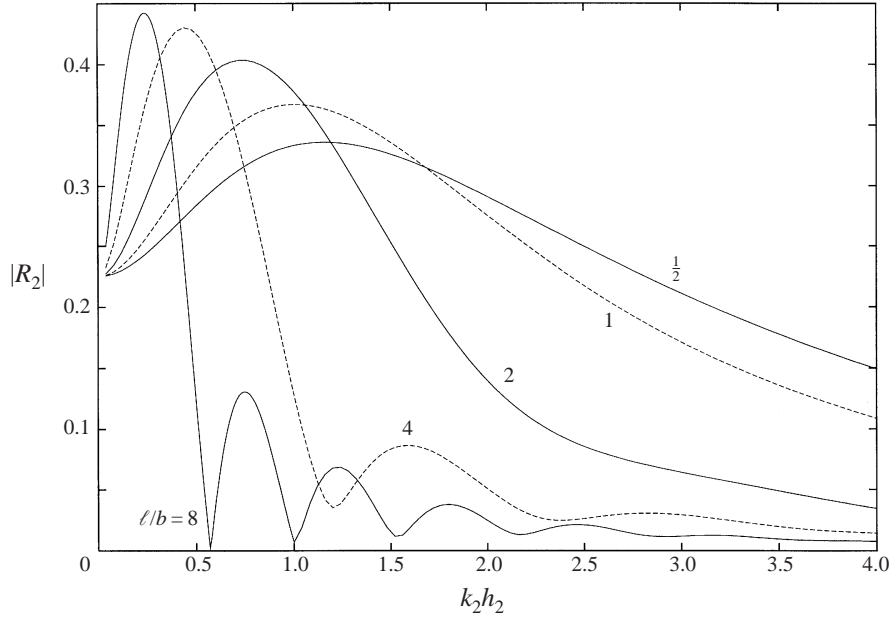


FIGURE 7. Reflection coefficient, $|R_2|$, against wavenumber k_2h_2 for the slope profiles given by $\hat{h}(x) = 1 - 3x^2 + 2x$ with $h_1/h_2 = \frac{2}{5}$, for different values of ℓ/b shown against the curves.

shown in figure 3(d), having a protrusion raised above the constant depth h_1 , there is a maximum in reflection coefficient, before dropping towards zero at higher frequencies. Unsurprisingly, the reflection is higher for this raised topography than from a vertical step over all frequencies. The lowest reflection in the set of curves shown in figure 6 arises in the case when $\alpha = 1$, corresponding to the bed shape illustrated in figure 3(e). Although the step joins the lower depth at an acute angle, the gentle gradient and smooth join to the shallower depth combines to give low reflection. For $\alpha = 0$, we have just recovered the plane slope and increased reflection occurs when the slope becomes increasingly convex as illustrated in the curve with $\alpha = -1$ (see figure 3f).

The final set of curves shown in figure 7 concentrates on the case of a quadratic profile with a raised protrusion defined by (6.5) with $h_1/h_2 = \frac{2}{5}$ and $\alpha = 3$ such that the minimum depth at the top of the protrusion is $\frac{1}{2}h_1$. Again, we consider the effect of the length of the bed on the reflection coefficient across a range of wavenumbers by varying ℓ/b between values of a half and eight. As the length of the bed increases, the peak in the reflection coefficient becomes sharper and larger and occurs at lower values of wavenumber.

We have also compared the reflection from a plane sloping bed that connects with the constant depths h_1 , h_2 at a corner and via small circular sections in order to determine the effect of local discontinuities in slope on the global quantities, such as the reflection coefficient. As expected, it was found that there is only a very small difference in reflection coefficient in these two cases.

A bed with a depression

In all cases where there is a depression below the depth h_2 , we non-dimensionalize the bed function by

$$\hat{h}(x) = (h_3 - h(x))/(h_3 - h_1)$$

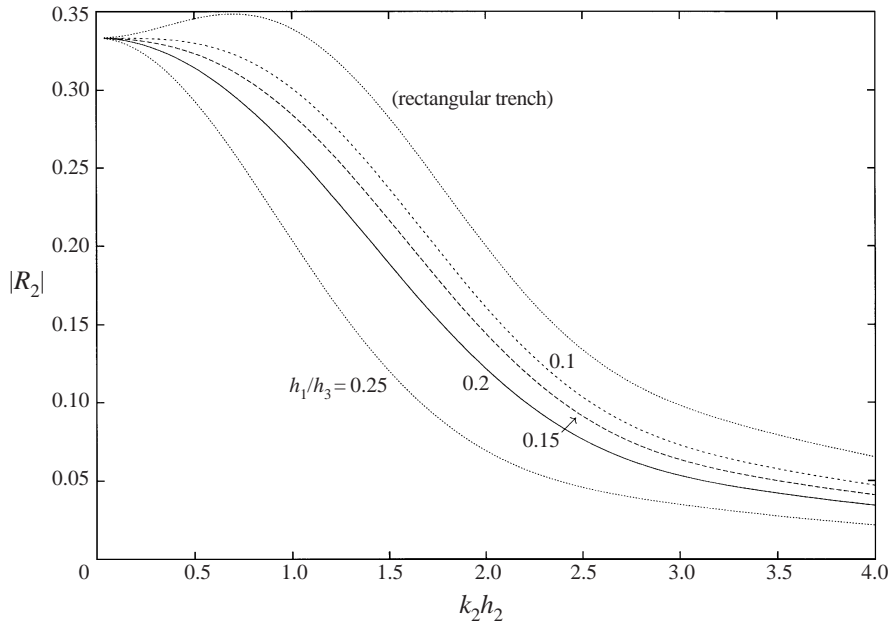


FIGURE 8. Reflection coefficient, $|R_2|$, against wavenumber k_2h_2 for the bed profiles $\hat{h}(x)$ defined in (6.6) with $h_1/h_2 = \frac{1}{4}$, $\ell/b = 1$ and for different values of h_1/h_3 shown against the curves.

such that $\hat{h}(0) = 1$, $\min_{0 \leq x \leq 1} \{\hat{h}(x) = 0\}$ and $\hat{h}(1) = \lambda$ where we define the parameter

$$\lambda = (h_3 - h_2)/(h_3 - h_1) = c/(b + c), \quad \text{where } c = h_3 - h_2$$

(see figure 2).

The convergence characteristics of $\tilde{\mathbf{Q}}_{ij}$ and $|R_i|$ in the case of a bed with a depression are the similar to the case of a bed without a depression described in detail at the beginning of this section when the extra truncation parameter controlling the number of expansion functions used on the interval $x = \ell$, $0 \leq y \leq h_2$ is chosen to be equal to N_1 . Notice that this more complicated method can also be applied to topography with no depression below the depth h_2 , and indeed, the depth h_3 can be chosen to be any value that exceeds the greatest fluid depth though there is little advantage in adopting such a course of action.

The simplest polynomial that dips to a depth h_3 below h_2 and joins both the depths h_1 and h_2 smoothly is a quartic, which is given in its non-dimensional form by

$$\hat{h}_4(x) = 1 - \alpha x^4 + (2\alpha + 2(1 - \lambda))x^3 - (\alpha + 3(1 - \lambda))x^2 \tag{6.6}$$

where α is defined to be the positive root of

$$16\alpha^3 - (\alpha + 3(1 - \lambda))^3(\alpha - (1 - \lambda)) = 0.$$

An illustration of a particular bed profile generated by (6.6) is given in figure 3(g). Using this profile, we present in figure 8 the effect of the depth of the depression in the case when $h_1/h_2 = \frac{1}{4}$ and for the depressions $h_1/h_3 = 0.25, 0.2, 0.15, 0.1$, the first of these corresponding to no depression. Also shown on figure 8 is a curve of the reflection coefficient for a rectangular trench with the dimensions $h_1/h_2 = \frac{1}{4}$ and $h_1/h_3 = 0.15$. The reflection from the rectangular trench computed from (4.22) is relatively insensitive to the depth of the trench in comparison with the smooth-joining

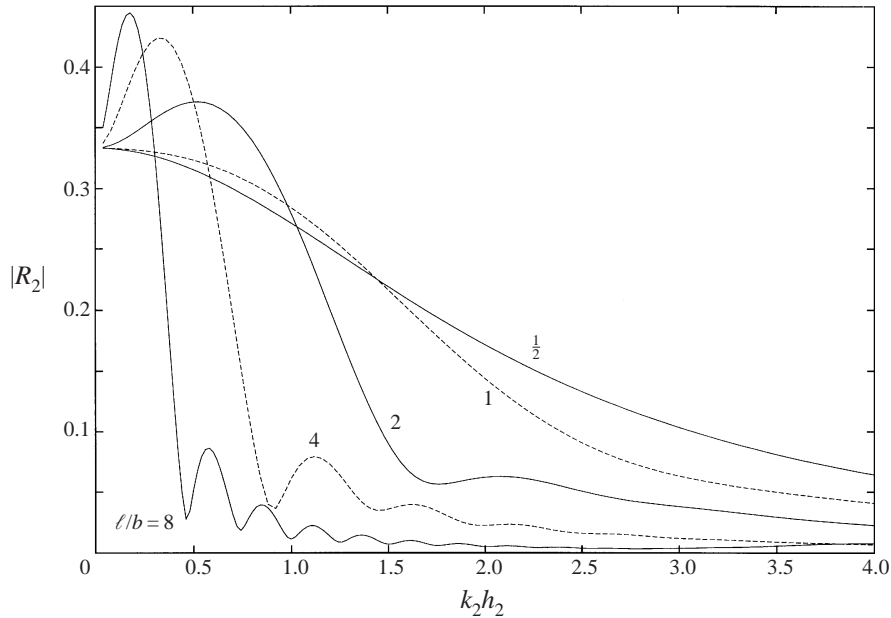


FIGURE 9. Reflection coefficient, $|R_2|$, against wavenumber $k_2 h_2$ for the bed profiles $\hat{h}(x)$ defined in (6.6) with $h_1/h_2 = \frac{1}{4}$, $h_1/h_3 = 0.15$ and for different values of ℓ/b shown against the curves.

quartic bed profile to the extent that curves for $h_1/h_3 < 0.15$ are indistinguishable from the curve for $h_1/h_3 = 0.15$. As the value of h_1/h_3 is reduced further below 0.1, the curves of reflection tend towards the curve for the rectangular trench.

Results obtained for other values of h_1/h_2 and other bed shapes also show similar variation of reflection coefficient with the depth of depression.

Of more interest are the curves of reflection coefficient against wavenumber for different bed lengths, shown in figure 9. Once more, we have used the smooth-joining quartic bed profile given by (6.6) with $h_1/h_2 = \frac{1}{4}$ and fixed the depth of the depression by setting $h_1/h_3 = 0.15$. It can be seen that as the bed length ℓ/b is increased from a half to eight, the behaviour for large enough wavenumbers is reminiscent of that already seen in figures 4 and 5 for bed profiles with no depression and no protrusion above the depth h_1 . Unlike these latter results, however, the effect of lengthening the bed with a depression at low wavenumbers is to increase the reflection to a maximum above its long-wave limiting value.

7. Conclusions

In this paper we have formulated the solution to the problem of the scattering of two-dimensional small-amplitude water waves by a step of arbitrary cross-section connecting two semi-infinite regions of constant fluid depth. Unlike many approaches to this particular problem, no approximation is made to the governing linearized water wave equations describing the fluid motion nor to the topography. The problem is formulated by choosing simple combinations of Green's functions appropriate to the various regions of constant fluid depth and using them in Green's identity. The key step is in the treatment of the contribution from the undulating part of the bed which uses the Cauchy–Riemann equations to transfer normal derivatives of certain functions to tangential derivatives of other functions. As a result the coupled

system of integral equations is self-adjoint and the kernels are at most logarithmically singular.

The case when the varying part of the bed, described by the function $y = h(x)$, dips to a maximum depth h_3 below the deeper of the constant levels, h_2 , has to be considered separately and requires the use of an additional Green's function associated with the constant depth h_3 . The formulation in both cases, however, is essentially the same.

The integral equations are in terms of unknown functions which are related to the horizontal fluid velocities across vertical planes above the joins of the step with the constant depths and the tangential fluid velocity along the step. The various reflection and transmission coefficients are contained in the four elements of a scattering matrix defined in terms of various inner products involving the unknown functions in the coupled integral equations. A variational approach equivalent to Galerkin's method is employed to approximate the solution to the integral equations and particular attention is paid to the choice of trial function which, by incorporating the physical behaviour of the fluid, results in rapid and accurate convergence with a small number of functions in the Galerkin expansion. Indeed, for most cases, less than five terms are required in the expansion to give results accurate to six decimal places. More terms are required for more complicated bed shapes and for higher frequencies. The accuracy of the results is independently confirmed using the more general case allowing for a depression of the bed below the lower of the two constant depths. Results obtained for topographies involving corners at the join with the constant depths illustrate the power of the variational method with the particular choice of functions used in the approximations to the solutions to the integral equations.

Throughout the paper we have described the topography in terms of a single-valued function $y = h(x)$. This is for convenience only, and other parametrizations of the topography are permitted. In particular, the method may be very easily adapted to include steps with overhanging lips by describing them as $x = h(y)$, $h_1 \leq y \leq h_2$.

The extension to oblique wave incidence is not obvious using the current approach, due to the use of the Cauchy–Riemann equations. However, the comments made at the end of §3 outline an alternative approach to the formulation of this problem which do not employ the Cauchy–Riemann equations and may, in principle, be successfully applied to oblique wave incidence.

Appendix. Calculation of e_{mn}

Instead of (5.15), we write

$$e_{mn} = \int_0^\ell v_m(x_0) \int_0^\ell v_n(x) \sum_{r=1}^{\infty} \frac{\chi_{2,r}(h(x))\chi_{2,r}(h(x_0))}{2k_{2,r}h_2} e^{-k_{2,r}|x-x_0|} dx dx_0.$$

Only one double integral needs be computed and the integrand is free from rapid oscillations. The kernel contains a logarithmic singularity along the line $x = x_0$. This is dealt with by subtracting the asymptotic leading-order contribution of the terms in the kernel and adding them back on.

Note first that $k_{2,r}h_2 \sim r\pi$ and $N_{2,r} \sim \frac{1}{2}$ as $r \rightarrow \infty$ and so

$$\chi_{2,r}(h(x)) \sim \sqrt{2} \sin\{r\pi(1 - h_1/h_2)\hat{h}(x/\ell)\}, \quad r \rightarrow \infty,$$

where $\hat{h}(x)$, defined in (6.1), is independent of ℓ , h_1 , h_2 and $\hat{h}(0) = 1$, $\hat{h}(1) = 0$. We re-write the infinite sum as

$$\sum_{r=1}^{\infty} \left[\frac{\chi_{2,r}(h(x))\chi_{2,r}(h(x_0))}{2k_{2,r}h_2} e^{-k_{2,r}|x-x_0|} - \frac{\sin\{r\pi(1-h_1/h_2)\hat{h}(x/\ell)\} \sin\{r\pi(1-h_1/h_2)\hat{h}(x_0/\ell)\}}{r\pi} e^{-r\pi|x-x_0|/h_2} \right] + \sum_{r=1}^{\infty} \frac{\sin\{r\pi(1-h_1/h_2)\hat{h}(x/\ell)\} \sin\{r\pi(1-h_1/h_2)\hat{h}(x_0/\ell)\}}{r\pi} e^{-r\pi|x-x_0|/h_2}. \quad (\text{A } 1)$$

The sum in the square brackets that converges for $0 \leq x, x_0 \leq \ell$ we call $S(x, x_0)$ and the corresponding integral is termed $e_{mn}^{(1)}$ such that

$$e_{mn}^{(1)} = \int_0^{\ell} v_m(x_0) \int_0^{\ell} v_n(x) S(x, x_0) dx dx_0. \quad (\text{A } 2)$$

The last term in (A 1) can be summed explicitly (Gradshteyn & Ryzhik 1981, § 1.462) to

$$\frac{1}{2\pi} \ln T(x, x_0), \quad (\text{A } 3)$$

where

$$T(x, x_0) = \left[\frac{\sin^2\{\frac{1}{2}\pi(1-h_1/h_2)(\hat{h}(x/\ell) + \hat{h}(x_0/\ell))\} + \sinh^2\{\pi/(2h_2)(x-x_0)\}}{\sin^2\{\frac{1}{2}\pi(1-h_1/h_2)(\hat{h}(x/\ell) - \hat{h}(x_0/\ell))\} + \sinh^2\{\pi/(2h_2)(x-x_0)\}} \right]^{1/2}. \quad (\text{A } 4)$$

This expression is singular in the denominator at $x = x_0$ and in the numerator at points $x = x_0$ such that $\hat{h}(x) = 0$, of which $x = x_0 = \ell$ is always such a point. Thus the factor in (A 3) contains the principal source-like behaviour of the Green's function: logarithmic singular at $x = x_0$ and also at $x = x_0$, $h(x) = h_2$ corresponding to the coalescence of the source point and the image point in the bed $y = h_2$.

The troublesome logarithmic singularities now reside in the integral

$$\frac{1}{2\pi} \int_0^{\ell} v_m(x_0) \int_0^{\ell} v_n(x) \ln [T(x, x_0)] dx dx_0 = e_{mn}^{(2)} + e_{mn}^{(3)},$$

where we write

$$e_{mn}^{(2)} = \frac{1}{2\pi} \int_0^{\ell} v_m(x_0) \int_0^{\ell} v_n(x) \ln[\ell^{-1}|x-x_0|T(x, x_0)] dx dx_0, \quad (\text{A } 5)$$

and

$$e_{mn}^{(3)} = -\frac{\ell^2}{2\pi} \int_0^1 v_m(\ell x_0) \int_0^1 [v_n(\ell x) - v_m(\ell x_0)] \ln|x-x_0| dx dx_0 - \frac{\ell^2}{2\pi} \int_0^1 v_n(\ell x) v_m(\ell x) [x \ln(x) + (1-x) \ln(1-x) - 1] dx. \quad (\text{A } 6)$$

The logarithmic singularity on $x = x_0$ has been suppressed by the introduction of the simple logarithmic factor in (A 5) and its reinstatement in (A 6) has been arranged in such a way that the singularities are integrated out analytically. We have not given explicit treatment to singularities arising in the kernel of (A 5) from values of x such

that $h(x) = h_2$. It turns out that these points cannot be integrated out explicitly in a simple manner, and must be dealt with numerically. Finally,

$$e_{mn} = e_{mn}^{(1)} + e_{mn}^{(2)} + e_{mn}^{(3)}.$$

Notice that $e_{mn}^{(3)}$ is in fact independent of all parameters, allowing it to be computed just once, whilst $e_{mn}^{(2)}$ is independent of frequency, and only needs to be calculated once for each geometrical configuration and applies over all wave frequencies.

REFERENCES

- ATHANASSOULIS, G. A. & BELIBASSAKIS, K. A. 1999 A consistent coupled-mode theory for the propagation of small-amplitude water waves over variable bathymetry regions. *J. Fluid Mech.* **389**, 275–301.
- BERKHOFF, J. C. W. 1972 Computation of combined refraction-diffraction. *Proc. 13th Conf. Coastal Engng, Vancouver*, vol. 2, pp. 471–490. ASCE.
- BERKHOFF, J. C. W. 1976 Mathematical models for simple harmonic linear waves. Wave diffraction and refraction. PhD thesis, Technical University of Delft.
- BOOIJ, M. 1983 A note on the accuracy of the mild-slope equation. *Coastal Engng* **7**, 191–203.
- BOYLES, C. A. 1984 *Acoustic Waveguides. Applications to Oceanic Science*. John Wiley.
- CHAMBERLAIN, P. G. & PORTER, D. 1995 The modified mild-slope equation. *J. Fluid Mech.* **291**, 393–407.
- DEVILLARD, P., DUNLOP, F. & SOUILLARD, B. 1988 Localization of gravity waves on a channel with a random bottom. *J. Fluid Mech.* **186**, 521–538.
- EVANS, D. V. 1972 The application of a new source potential to the problem of transmission of water waves over a shelf of arbitrary profile. *Proc. Camb. Phil. Soc.* **71**, 391–410.
- EVANS, D. V. & FERNYHOUGH, M. 1995 Edge waves along periodic coastlines. Part 2. *J. Fluid Mech.* **297**, 307–325.
- EVANS, D. V. & LINTON, C. M. 1991 Trapped modes in open channels. *J. Fluid Mech.* **225**, 153–175.
- EVANS, D. V. & LINTON, C. M. 1994 On step approximations for water-wave problems. *J. Fluid Mech.* **278**, 229–249.
- FAWCETT, J. A. 1992 A derivation of the differential equations of coupled-mode propagation. *J. Acoust. Soc. Am.* **92**, 290–295.
- FERNYHOUGH, M. & EVANS, D. V. 1995 Scattering by a periodic array of rectangular blocks. *J. Fluid Mech.* **305**, 263–279.
- FITZ-GERALD, G. F. 1976 The reflexion of plane gravity waves travelling in water of variable depth. *Phil. Trans. R. Soc. Lond. A* **284**, 49–89.
- GRADSHTEYN, I. S. & RYZHIK, I. M. 1981 *Tables of Integrals, Series and Products*. Academic.
- GUAZZELLI, E., REY, V. & BELZONS, M. 1992 Higher-order Bragg reflection of gravity surface waves by periodic beds. *J. Fluid Mech.* **245**, 301–317.
- KIRBY, J. T. 1986 A general wave equation for waves over rippled beds. *J. Fluid Mech.* **162**, 171–186.
- KREISEL, G. 1949 Surface waves. *Q. Appl. Maths* **7**, 21.
- LAMB, H. 1932 *Hydrodynamics*. Cambridge University Press.
- LUI, P. L.-F. & LIGGETT, J. A. 1982 Applications of boundary element methods in problems of water waves. In *Developments in Boundary Element Methods – 2* (ed. P. K. Banerjea & R. P. Shaw). London: Applied Science.
- MASSEL, S. R. 1993 Extended refraction–diffraction equation for surface waves. *Coastal Engng* **19**, 97–126.
- MEI, C. C. 1978 Numerical methods in water-wave diffraction and radiation. *Ann. Rev. Fluid Mech.* **10**, 393–416.
- MILES, J. W. 1967 Surface wave scattering matrix for a shelf. *J. Fluid Mech.* **28**, 755–767.
- O'HARE, T. J. & DAVIES, A. G. 1991 A new model for surface wave propagation over undulating topography. *Coastal Engng* **18**, 251–266.
- PORTER, D. & CHAMBERLAIN, P. G. 1997 Linear wave scattering by two-dimensional topography. In *Gravity Waves in Water of Finite Depth* (ed. J. N. Hunt), pp. 13–53. Southampton, Computational Mechanics.

- PORTER, D. & STAZIKER, D. G. 1995 Extension of the mild-slope equation. *J. Fluid Mech.* **300**, 367–382.
- PORTER, R. 1995 Complementary methods and bounds in linear water waves. PhD thesis, University of Bristol, UK.
- PORTER, R. & EVANS, D. V. 1995 Complementary approximations to wave scattering by vertical barriers. *J. Fluid Mech.* **294**, 155–180.
- REY, V. 1992 Propagation and local behaviour of normal incident gravity waves over varying topography. *Eur. J. Mech. B: Fluids* **11**, 213–232.
- ROSEAU, M. 1976 *Asymptotic Wave Theory*. North-Holland.
- RUTHERFORD, S. R. & HAWKER, K. E. 1981 Consistent coupled mode theory of sound propagation for a class of nonseparable problems. *J. Acoust. Soc. Am.* **70**, 554–584.
- SMITH, R. & SPRINKS, T. 1975 Scattering of surface waves by a conical island. *J. Fluid Mech.* **72**, 373–384.
- STAZIKER, D. J., PORTER, D. & STIRLING, D. S. G. 1996 The scattering of surface waves by local bed elevations. *Appl. Ocean Res.* **18**, 283–291.